ABSTRACT

STUDIES ON MULTIPORT DIFFUSER OF UNIFORM LATERAL MOMENTUM

Edward Oi-Wah Ng

The manifold which is being studied in this Report was originally designed to ensure uniform distribution of lateral momentum. The present study is concerned with the distribution of lateral momentum when the length of the manifold extended or shortened at the upstream end or the downstream end. The change in length of the manifold may be required for varying the design discharge capacity. In the present experimental arrangement, the open downstream end simulated the condition of extending the manifold to provide additional discharging capability.

The analysis of a manifold with uniform lateral openings has been developed in the past. Its result can be utilized in analysing the manifold described above, which has nonuniform lateral openings. The hypothesis is that for short pipes, where the frictional effects are negligible, the flow in each lateral discharge opening will not be affected by varying the spacing in between the openings, assuming that the average pressure regain coefficient γ and lateral discharge resistance H will remain constant . This is expected to be true for hole spacings which exceed a critical value. Such a critical value can be

obtained from an experimental program. The flow in each hole of a manifold of uniform distribution of openings is first calculated by using the equation which has been long established. Sebsequently, the distribution of discharge can be obtained by arranging the holes to resemble the desired outlet distribution. This analysis is suitable for short manifolds because friction is being neglected. The results of the test agree reasonably well with the analysis.

ACKNOWLEDGEMENTS

ACKNOWLEDGEMENTS

The author wishes to express his gratitude to Professor A.S. Ramamurthy of the Department of Civil Engineering at Concordia University (Sir George Williams Campus), Montreal, for suggesting the topic for this project.

The assistance of Mr. M.G. Satish in this project is thankfully acknowledged.

TABLE OF CONTENTS

TABLE OF CONTENTS

LIST OF TABLES

LIST OF TABLES

LIST OF FIGURES

LIST OF FIGURES

NOMENCLATURE

NOMENCLATURE

A	Cross-sectional area of manifold
A_L	Area of lateral opening per unit length
D	Diameter of manifold
f	Friction coefficient of pipe wall
L_1	Length of manifold inch
P	Pressure
$Q(x)$	Flow in manifold at point x
ρ	Density of fluid
γ	Pressure regain coefficient
H	Flow resistance of the branch
Q_o	Inlet flow at upstream
r	Downstream flow ratio $Q(L)/Q_o$
q_i	Flow in $i^{\underline{th}}$ hole
V	Flow speed in manifold
v	Flow speed in branch

CHAPTER I

INTRODUCTION

CHAPTER 1

INTRODUCTION

1.1 STATEMENT OF THE PROBLEM

Studies by Robillard [1] indicate that by injecting the effluent as a counter jet into a main stream, a vortex sheet can be generated to provide an effective means of jet mixing on a large scale. The characteristics of the vortex sheet of the counter jet are governed by J/U^2, where J is the kinematic momentum of the jet, and U is the velocity of the main stream. In order to ensure an effective dilution along the diffuser, the kinematic momentum per unit length has to be maintained uniform. Satish [2] designed a manifold based on this criterion of uniform lateral momentum with a closed downstream end (Figure 1.1).

The characteristics of flow in a discharge manifold which has a closed downstream end has been investigated in the last few decades. However, a manifold with the downstream end partially opened is seldom studied. If the manifold described above is needed to be extended or shortened to accept the charges in the design discharge capacity, the uniformity of lateral momentum along the existing manifold must also be maintained. In the experiments, manifolds of various effective lengths which had an open downstream end have been tested.

The differential equation denoting the flow through the lateral outlets of a manifold with nonlinear area distribution is difficult to solve. Hence, a simplified analysis is derived utilizing the analysis for the manifold with uniform lateral openings to being with. A hypothesis is made that any change in hole spacings will not affect the discharge of each hole. This hypothesis is not unreasonable if friction is not a dominant factor, as in short pipes. If the hole spacings are too close, the variation in the pressure regain coefficient with respect to the hole spacing any strongly influence the test results. However, one can obtain a general picture showing the effects of the downstream flow and the effect of extending or shortening the manifold on the flow pattern, for all cases where the hole spacings do not alter the pressure regain coefficient.

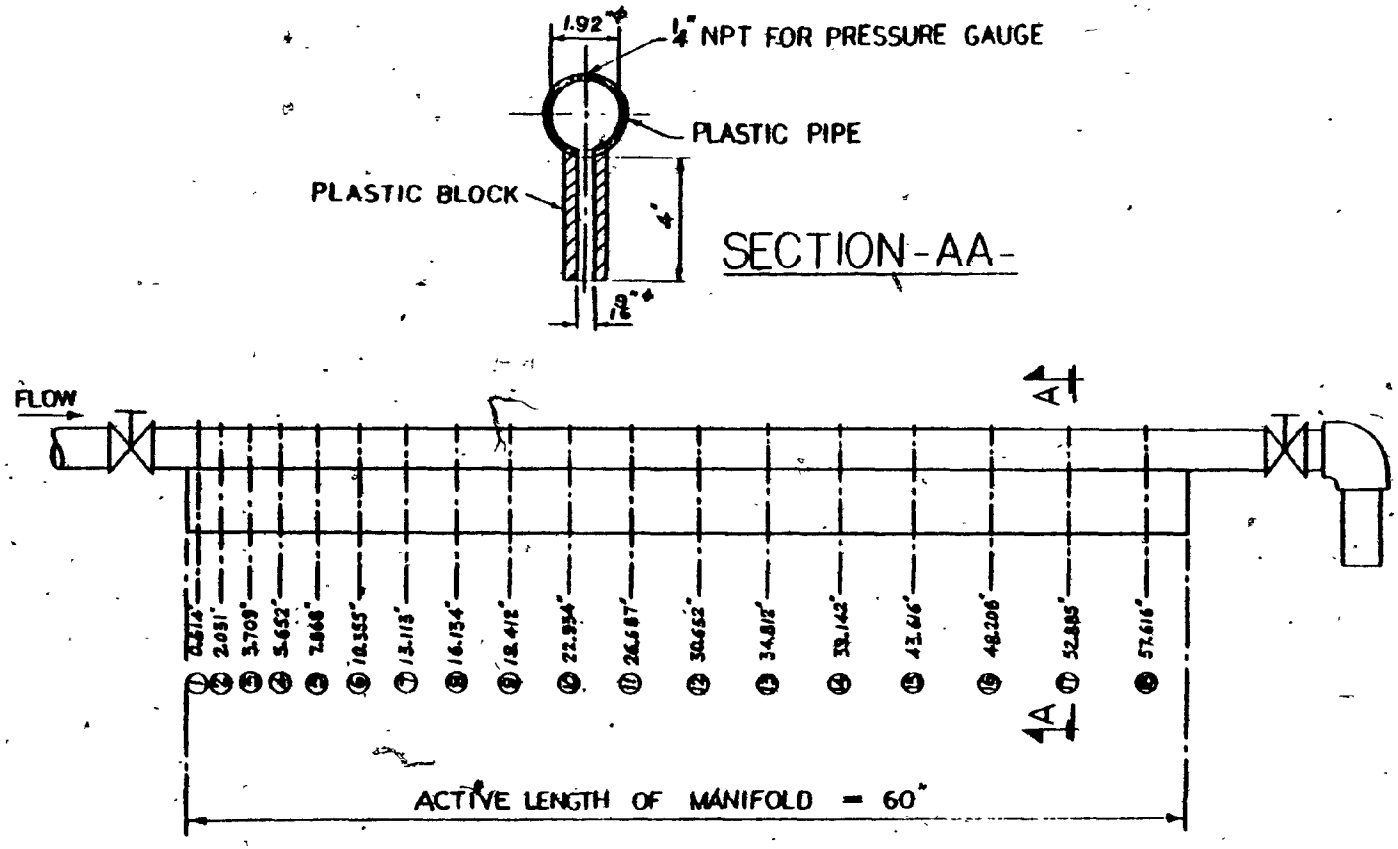

FIG. 1.1 ASSEMBLY OF THE MANIFOLD TESTED

CHAPTER II

A REVIEW OF PREVIOUS STUDIES

CHAPTER II

A REVIEW OF PREVIOUS STUDIES

Keller [3] analyzed several types of manifolds on the basis of two factors:

1) Inertia, and
2) Friction

to determine the flow characteristics.

He suggested that there were two parameters which defined a manifold, namely, the ratio of active length of a manifold to its diameter, or L/D, and the area ratio or sum of areas of discharge openings/cross-sectional area of the manifold. It was pointed out that a larger L/D would allow a larger area ratio for a uniform discharge. But the area ratio changes did not affect the flow in a manifold of variable cross-sectional area.

Dow [4] considered the cases for laminar flow and turbulent flow in a manifold. He introduced a constant α to the term of momentum in the differential equation. According to Dow, the distribution of lateral discharge depends upon the area ratio L/D, and the incoming flow Q_o.

McNown [5] presented a thorough study of the flow characteristics at a branch point in a closed conduit. He observed from the experiments that for small ratios of branch

flow to main flow = Q_3/Q_1, the head loss in the conduit at the branch point was negative. This was explained in terms of the non-uniform velocity profile. The ratio of discharge-opening diameter to conduit diameter D_3/D_1, was considered to have only a slight effect upon the pressure recovery. However, the spacing of branch points was found to affect the pressure recovery pattern.

Horlock [6] investigated the flow in discharge manifolds with open or closed downstream ends. He concluded that a value of (V/b), i.e., the ratio of velocity along the manifold to the normal discharge velocity, should be reached, far from the end of the manifold, which was only the function of fa/b, where f was the skin friction factor and a/b the area ratio. This value of (V/b) was independent of the discharge end being open or closed.

Haerter [7] studied the characteristics of manifold flow along branched air-ducts. It was noted that the pressure regain coefficient depended upon the velocity profile in the manifold.

In the case of a short conduit, with constant cross-sectional area and equally-spaced branch, where the friction is negligible, the distribution of discharge was determined by the parameters A_s and B_s, where

$$A_s = \frac{\text{effective branch area}}{\text{cross-sectional area of duct}}$$

$$B_s = \sqrt{\text{pressure regain coefficient} \times \text{coefficient of loss at the fitting}}$$

If $A_s B_s > 1.57$ (i.e. $\pi/2$), there would be no outflow along the upstream section of the duct until it reached a point downstream, from where on, the remaining area ratio A_s would give $A_s B_s < 1.57$.

Vigander et al [8] analysed the flow in a corrugated discharge diffuser for Browns Ferry Nuclear Power Plant, using the step-by-step method. For a small (d/D), the diameter ratio, and a large ratio of pipe diameter to height of corrugation, the experiments showed that the discharge coefficient was mainly affected by the ratio of velocity head to the total head. The other geometric parameters had no discernible effect upon the orifice discharge characteristics.

Bajura [9] used the momentum equation to analyse the flow in a manifold. He presented graphical data for the static pressure regain coefficient and the turning loss coefficient which was being included in the momentum equation. Both coefficients were affected by branch spacing, the diameter-to-length ratio and the ratio of discharge-to-main flow (Q_s/Q). In the case of negligible friction, the discharge distribution of a manifold of uniform lateral openings was related to these

parameters namely:

1) The area ratio,

2) the resistance at the branch, and

3) the static pressure regain coefficient.

Berlamont et al [10] analysed the lateral outflow in perforated conduits for three different pipe flow conditions, namely:

1) Laminar flow,

2) turbulent smooth flow, and

3) turbulent rough flow.

The discharge through the branch was described by a general power-law. It was shown that the lateral outflow was mainly governed by:

1) The velocity distribution correction coefficient,

2) the friction $(f\frac{L}{D})$, and

3) $\frac{U_o^2}{2gh_o}$,

where

U_o = the initial velocity in the conduit, and

h_o = the initial static head.

Hudson et al [11] collected numerous published experimental data to devise simplified graphical solutions for the hydraulic changes associated with the dividing flow branch points. For square-edged laterals, they found that

$$\frac{h'}{(V_L^2/2g)} = \phi \left(\frac{V_m}{V_L}\right)^2 + \theta$$

where

h' = lateral entry loss

V_L = lateral outflow velocity

V_m = main conduit velocity

and for the lateral length

$L > 3D$ $\theta = 0.4$ $\phi = 0.9$ (long lateral)

$L < 3D$ $\theta = 0.7$ $\phi = 1.67$ (short lateral)

The pressure recovery could be estimated from the graph of

$$\frac{\Delta h}{V_m^2/2g} \geq \frac{V_{m+1}}{V_m}$$

for design purposes.

CHAPTER III

SET-UP AND PROCEDURES OF THE TEST

CHAPTER III

SET-UP AND PROCEDURES OF THE TEST

3.1 SET-UP OF THE EXPERIMENT

The manifold tested was a PVC pipe of 2" diameter. A PVC block was glued to the pipe and eighteen holes of 9/16" diameter were drilled in the pipe-block system at prescribed locations. Taps for pressure gauges were located diametrically opposite to each of the lateral openings. There was a valve at each end of the manifold for controlling the inflow and the downstream flow. A movable scale was used for weighing the lateral discharge collected. The original manifold with 18 holes and 60" long, is shown in Figure 3.1.

3.2 TESTING PROCEDURES

The manifold was tested with different numbers of holes or different active lengths, and the various downstream flows as shown in Table 3.1. In the shortened manifolds, either upstream or downstream lateral openings were plugged from the original eighteen holes.

For manifold with hole numbers 1-18, 3-18 and 5-18, the downstream flows could be of any value, since the uni-

formity of the lateral momentum could not be achieved with the existence of downstream flow. The purpose of testing the manifolds of these configurations was to study how the flow pattern was being affected by the down-stream flow.

For manifolds with hole numbers 1-16 and 1-14, the downstream flows were adjusted for two conditions:

1) The uniform lateral momentum, and

2) the zero lateral flow that occurred in the first hold upstream.

For every test, before the measurement was made, water was allowed to circulate for a while, to let the transients decay.

The discharge of each lateral opening and the down-stream flow were measured separately. The discharge was guided by a steel chamber to the scale. The time interval for 200 lbs or 100 lbs of water was recorded for calculating the discharge rate.

TABLE 3.1 NUMBER OF TESTS FOR DIFFERENT MANIFOLD ASSEMBLIES

No. of Holes	Hole No.	With Downstream Closed	With Downstream Open
18	1-18	1	1
16	1-16	1	2
16	3-18	0	1
14	1-14	1	2
14	5-18	0	1

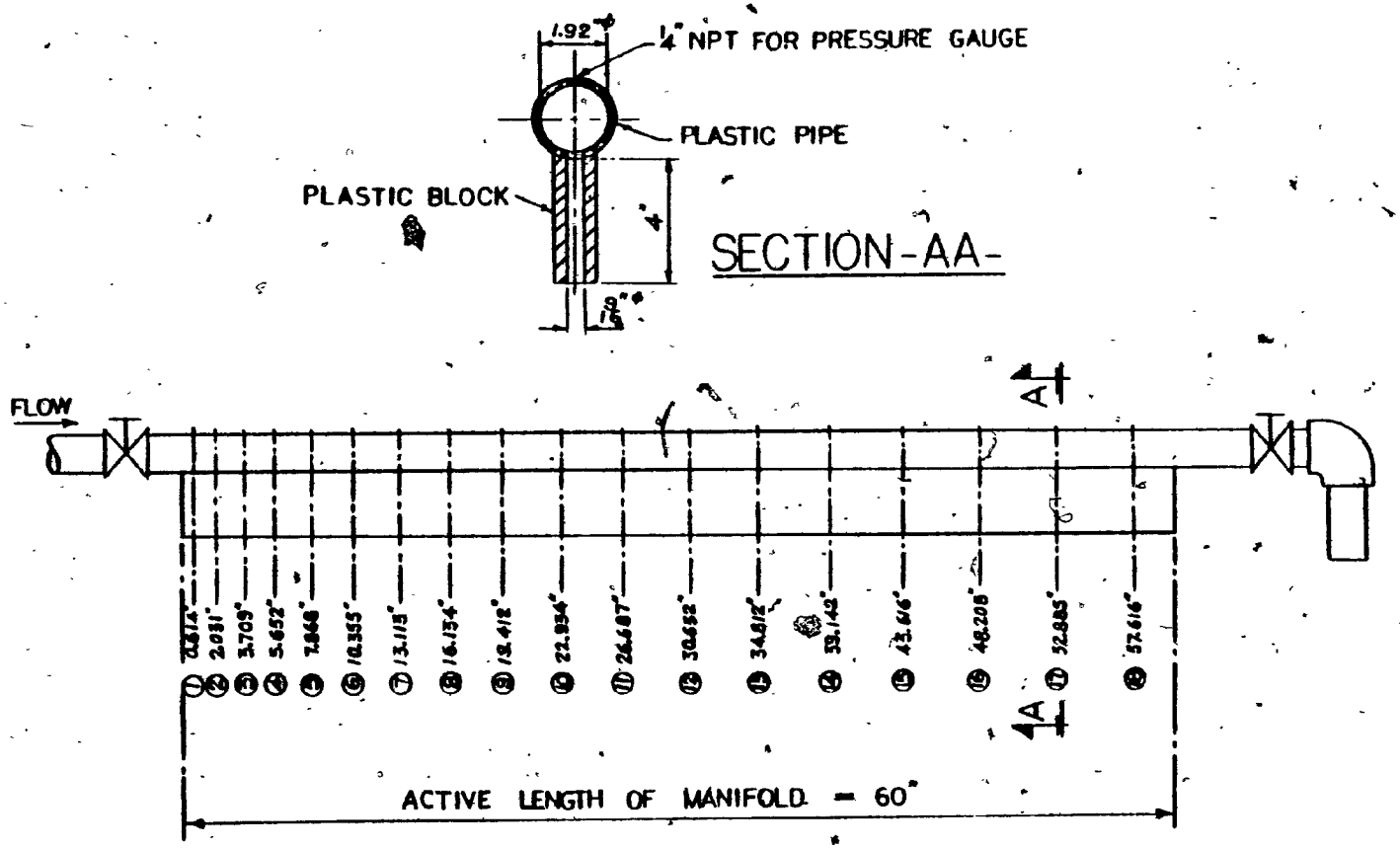

FIG. 3.1 ASSEMBLY OF THE MANIFOLD TESTED

CHAPTER IV

ANALYSIS

CHAPTER IV

ANALYSIS

From the previous studies [7],[9], the general equation governing the manifold flow is as follows:

$$\frac{1}{\rho}\frac{dP}{dX} + \frac{f}{2D}V^2 + 2V\frac{dV}{dX} + \gamma V v \frac{A_L(X)}{A} = 0 \qquad (4.1)$$

where

V = flow velocity in manifold

v = flow velocity in lateral branch

$A_L(X)$ = lateral opening per unit length

A = cross-sectional area of manifold

D = diameter of manifold

γ = pressure recovery factor

f = pipe friction factor

ρ = density of fluid

A particular case of Equation (4.1), which involves the additional condition of uniform lateral momentum along the span of the manifold, is derived in [2], and is given below.

$$(Q^*)'' - \frac{fL}{2D}\left(\frac{MR^2}{H}\right)^2 (Q^*)^2 [(Q^*)']^3 - (2-\gamma)\left(\frac{MR^2}{H}\right)(Q^*)[(Q^*)']^4 = 0 \qquad (4.2)$$

with the end conditions $Q^*(0) = 1$, $Q^*(1) = 0$,

where,

$Q^* = Q/Q_o$

$X^* = X/L$

Q_o = inlet flow

L = active length of manifold

MR = inflow momentum/total lateral momentum

The same manifold with different end conditions is being studied in the present report. When the end conditions of Equation (4.2) as described above varies, the uniformity of the distribution of lateral momentum cannot be maintained. In this case, only Equation (4.1) is applicable for the analysis. To solve Equation (4.1), in which the lateral area was found in [2] to be nonuniform, numerical methods can be adopted. However, a simpler method is suggested for the analysis, and the results describe the flow behaviour in a more comprehensive manner. To simplify the analysis, two assumptions are made, as follows:

1) For short manifolds, frictional loss is small. The tested model with L/D = 31.25 (for 18 holes), is considered to be short. Further, the pressure recovery head is much larger than the friction head. Hence, friction loss is neglected in the analysis presented herein.

2) The analysis is based on the hypothesis that in a frictionless manifold as shown in Figure 4.1, the lateral discharges q_1 and q_2 in Figure 4.1(a) will be the same as in Figure 4.1(b), regardless of the hold spacing, provided that the inlet condition remains unchanged. The flow resistance H and the pressure recovery factor γ at the branches are assumed to be unaffected by the hole spacing.

For simplicity, a manifold of uniform lateral opening will be used as the analytical model in the analysis. The flow and the discharge of each hole are first obtained from this analytical model. The flow and the discharge of the tested model can then be established by adjusting the hole spacings to resemble the manifold tested. Based upon this transformation, the flow characteristic of the analytical model with 18 holes and a closed downstream end will give the tested model a uniform lateral momentum. This particular flow characteristic from the analytical model will be used as the reference flow characteristic. One can predict whether a manifold will have uniform lateral momentum just by comparing the flow characteristic from its corresponding analytical model with the reference flow characteristic without transforming the analytical result.

For the simplified analytical model, Equation (4.1) becomes

$$Q'' + \frac{2-\gamma}{H}\left(\frac{A_L}{A}\right)^2 Q = 0 \qquad (4.3)$$

where

A_L = the lateral area per unit length

= constant

a) Manifold with closed downstream end.

From Equation (4.3), the flow and the discharge are given below.

$$\left.\frac{Q(X)}{Q_o}\right|_c = \frac{1}{\sin m_1} \sin m_1 \left(1-\frac{X}{L_1}\right) \qquad (4.4)$$

$$\left.\frac{Q'(X)}{Q_o}\right|_c = \frac{-m_1}{L_1 \sin m_1} \cos m_1 \left(1-\frac{X}{L_1}\right) \qquad (4.5)$$

where,

$$m_1 = \sqrt{\frac{2-\gamma}{H}}\ \frac{A_{T1}}{A}$$

and

A_{T1} = the total lateral area for length L_1, and

Subscript C = the case for closed downstream.

Let

$$\frac{X}{L_1} = \frac{1}{A_{T1}} \int_0^X A_L\, dx \qquad (4.6)$$

and

$$1 - \frac{X}{L_1} = \frac{1}{A_{T1}} \int_X^{L_1} A_L\, dx \qquad (4.7)$$

Substituting Equations (4.6) and (4.7) into Equations (4.4) and (4.5), one obtains

$$\frac{Q(X)}{Q_o} = \frac{1}{\sin m_1} \sin K \int_x^{L_1} A_L \, dx \quad (4.8)$$

$$\frac{Q'(X)}{Q_o} = \frac{-m_1}{L_1 \sin m_1} \cos K \int_x^{L_1} A_L \, dx \quad (4.9)$$

where,

$$K = \sqrt{\frac{2-\gamma}{H}} \frac{1}{A}$$

One can see from Equations (4.8) and (4.9), that the discharge at point X depends upon the integral of the lateral area from X to the downstream end L_1. Hence, if the manifold is shortened at the upstream, as shown in Figure 4.2, the flow characteristics along the new span will remain unchanged. The tested model which is shortened at the upstream will still have the uniform lateral momentum, and the change in the inlet flow Q_o only affects the magnitude of the lateral momentum, but not the uniformity.

In the case where the manifold is shortened at its downstream end to a new length L_3, as shown in Figure 4.3, the original (or reference) discharge along curve (a) is as described by Equation (4.8). The discharge for the shorter manifold along curve (b) is given by equation (4.10).

$$Q'(X)_3 = -\frac{Q_{o3}\, m_3}{\ell_3 \sin m_3} \cos K\left({}_x\int^{L_3} A_L\, dx\right)$$

$$= -\frac{Q_{o3}\, m_3}{\ell_3 \sin m_3} \cos K\left({}_x\int^{L_1} A_L\, dx - {}_{L_3}\int^{L_1} A_L\, dx\right) \qquad (4.10)$$

where,

Subscript 3 denotes the shorter manifold

Even though curve (b) can be scaled up or down to (b') by adjusting the inflow, it still cannot match with the reference curve (a) because of the phase shift ${}_{L_2}\int^{L_1} A_L\, dx$, in Equation (4.10). Hence, one can conclude that if the manifold (tested model) with a closed downstream end is shortened at the downstream end, the lateral momentum is no longer uniform.

b) Manifold with downstream end partially opened.

The end conditions are $Q(0) = Q_o$ and $Q(L_1) = rQ_o$. Then the solution equations for Equation (4.3) are

$$\frac{Q(X)}{Q_o} = \frac{1}{\sin m_1}\left(\sin m\,(1-\frac{X}{L_1}) + r\sin m\,\frac{X}{L_1}\right) \qquad (4.11)$$

$$\frac{Q'(X)}{Q_o} = -\frac{m_1}{L_1 \sin m_1}\left(\cos m\,(1-\frac{X}{L_1}) - r\cos m\,\frac{X}{L_1}\right) \qquad (4.12)$$

Substituting Equations (4.6) and (4.7) into Equations (4.11) and (4.12), one obtains the following equations:

$$\frac{Q(X)}{Q_o} = \frac{1}{\sin m_1} \left(\sin K \int_x^{L_1} A_L \, dx + \right.$$

$$\left. + r \sin K \int_o^x A_L \, dx\right) \qquad (4.13)$$

$$\frac{Q'(X)}{Q_o} = -\frac{m_1}{L_1 \sin m_1} \left(\cos K \int_x^{L_1} A_L \, dx - \right.$$

$$\left. - r \cos K \int_o^x A_L \, dx\right) \qquad (4.14)$$

where

$$K = \sqrt{\frac{2-\gamma}{H}} \frac{1}{A}$$

For the case of opened downstream end, the lateral discharge along the manifold is reduced by the occurrence of the downstream flow by the amount of $r \cos K \int_o^x A_L \, dx$, as shown in Equation (4.14).

It is noticed in Figure 4.4, that as the value of downstream flow ratio r increases to r_c, there will be no discharge at the upstream end, i.e., $Q'(0) = 0$. Under this condition, Equation (4.14) becomes

$$-\frac{m_1}{L_1} \frac{1}{\sin m_1} \left[\cos K \int_o^{L_1} A_L \, dx - r_c \cos K \int_o^o A_L \, dx\right] = 0$$

Therefore,

$$r_c = \cos K \int_0^{L_1} A_L \, dx$$

$$= \cos(K A_{T1}) \qquad (4.15)$$

One can see from Figure 4.4, that the uniformity of lateral momentum of manifold tested can no longer be maintained while there is a downstream flow.

In the previous section, it was found that the discharge can be increased by shortening the manifold at the downstream end. Figure 4.5(a) shows that the drop in discharge due to the existence of the downstream flow can be compensated by reducing the length of the manifold from the downstream end. In Figure 4.5(a), let the length of the shorter manifold be ℓ_3 and let $r = r^*$, such that

$$\left.\frac{Q'(X)_1}{Q(0)_1}\right|_c = \left.\frac{Q'(X)_3}{Q(0)_3}\right|_o \qquad (4.16)$$

where,

Subacripts C = closed downstream end

0 = opened downstream end

1 = the original manifold

3 = the manifold which is shortened at the downstream end

Substituting Equations (4.5) and (4.12) into Equation (4.16), we have

$$-\frac{m_1}{L_1 \sin m_1}\cos m_1\left(1-\frac{X}{L_1}\right) = -\frac{m_3}{\ell_3 \sin m_3}\left(\cos m_3\left(1-\frac{X}{\ell_3}\right) - r^* \cos m_3 \frac{X}{\ell_3}\right)$$

where,

$$0 \leq X \leq L_3$$

Since

$$\frac{m_1}{L_1} = \frac{m_3}{\ell_3} = \sqrt{\frac{Q-\gamma}{H}}\,\frac{A_L}{A}$$

Therefore,

$$\frac{\sin m_3}{\sin m_1}\cos m_1\left(1-\frac{X}{L_1}\right) = \cos m_3\left(1-\frac{X}{\ell_3}\right) - r^* \cos m_3 \frac{X}{\ell_3}$$

$$r^* = \left[\cos m_3\left(1-\frac{X}{\ell_3}\right) - \frac{\sin m_3}{\sin m_1}\cos m_1\left(1-\frac{X}{L_1}\right)\right]\frac{1}{\cos m_3 \frac{X}{\ell_3}}$$

$$= \left(\cos m_3 - \frac{\sin m_3}{\sin m_1}\cos m_1\right) + \tan \frac{m_3 X}{\ell_3}\left(\sin m_3 - \sin m_1 \frac{\sin m_3}{\sin m_1}\right)$$

$$= \left(\cos m_3 - \frac{\sin m_3}{\sin m_1}\cos m_1\right)$$

$$= \frac{\sin m_1 (1-m_3/m_1)}{\sin m_1}$$

Since

$$\frac{m_3}{m_1} = \frac{\ell_3}{L_1}$$

Therefore,

$$r^* = \frac{\sin m_1(1-\ell_3/L_1)}{\sin m_1} \qquad (4.17)$$

Compare Equation (4.15) to Equation (4.4)

$$r^* = \left.\frac{Q(L_3)_1}{Q(0)_1}\right|_c \qquad (4.18)$$

The result of Equation (4.18) shows that for the shortened manifold, if the downstream flow ratio r at $X = L_3$ is the same as the flow ratio at $X = L_3$ in the original manifold with a closed downstream end, the distribution of discharge along ℓ_3 in the shortened manifold will be the same as the original one. The uniformity of the lateral momentum can be maintained.

For another case, as shown in Figure 4.5(b), to shorten the manifold at upstream end, will not help to eliminate the effect of the downstream flow. In this case, the distribution of the lateral momentum will not be uniform. Instead, it tends to increase towards the downstream end.

NOTE: - Appendix I shows the derivation of Equations (4.3), (4.4), (4.5), (4.11) and (4.12). The values of r_c for 18 holes, 16 holes and 14 holes are also included in that section.

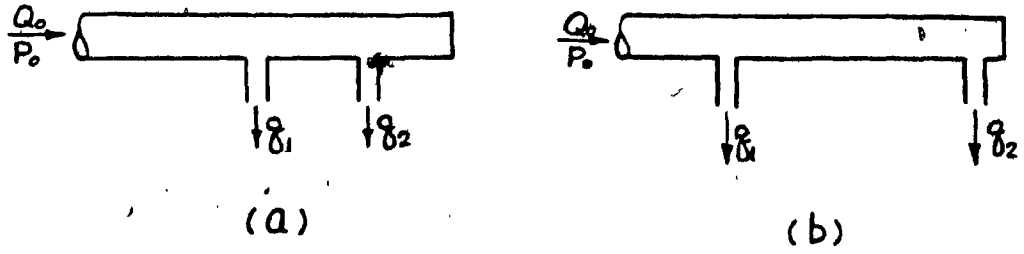

FIG. 4.1 MANIFOLDS OF DIFFERENT HOLE SPACINGS

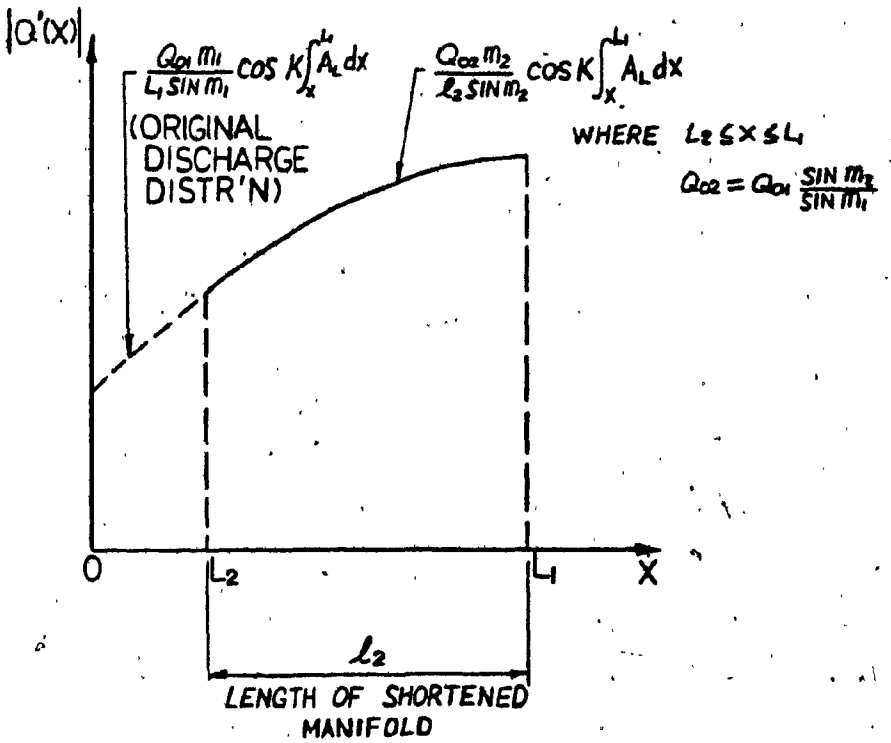

FIG. 4.2 DISCHARGE OF MANIFOLD WHICH IS SHORTENED AT THE UPSTREAM END WITH A CLOSED DOWNSTREAM END

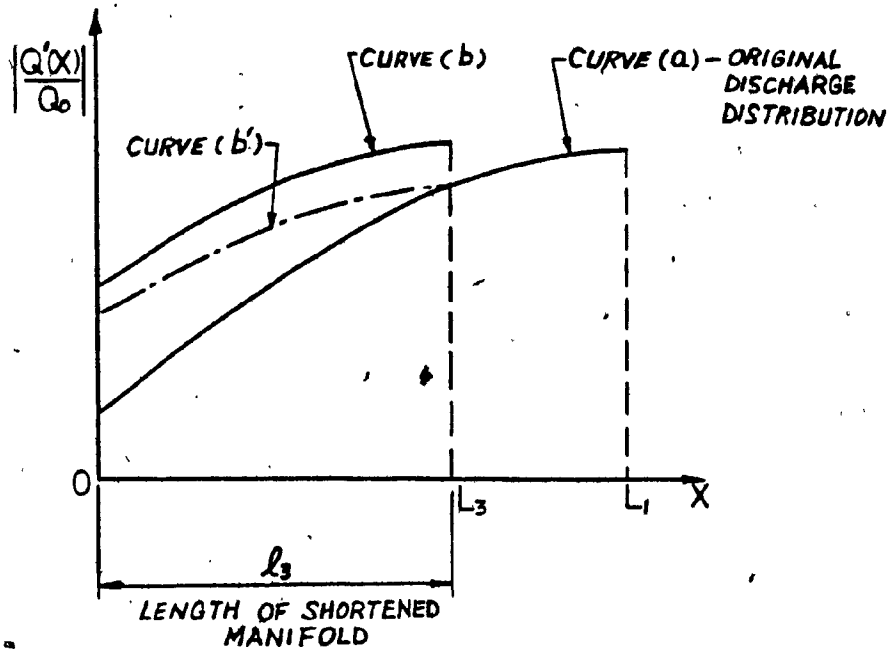

FIG. 4.3 DISCHARGE OF MANIFOLD WHICH IS SHORTENED AT THE DOWNSTREAM END WITH A CLOSED DOWNSTREAM END

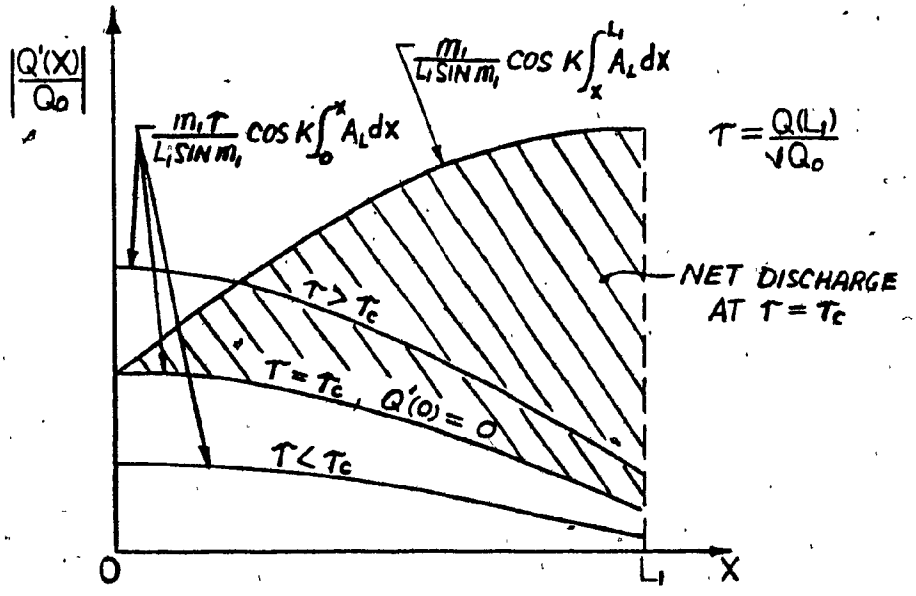

FIG. 4.4 DISCHARGE OF A MANIFOLD WITH DOWNSTREAM FLOW

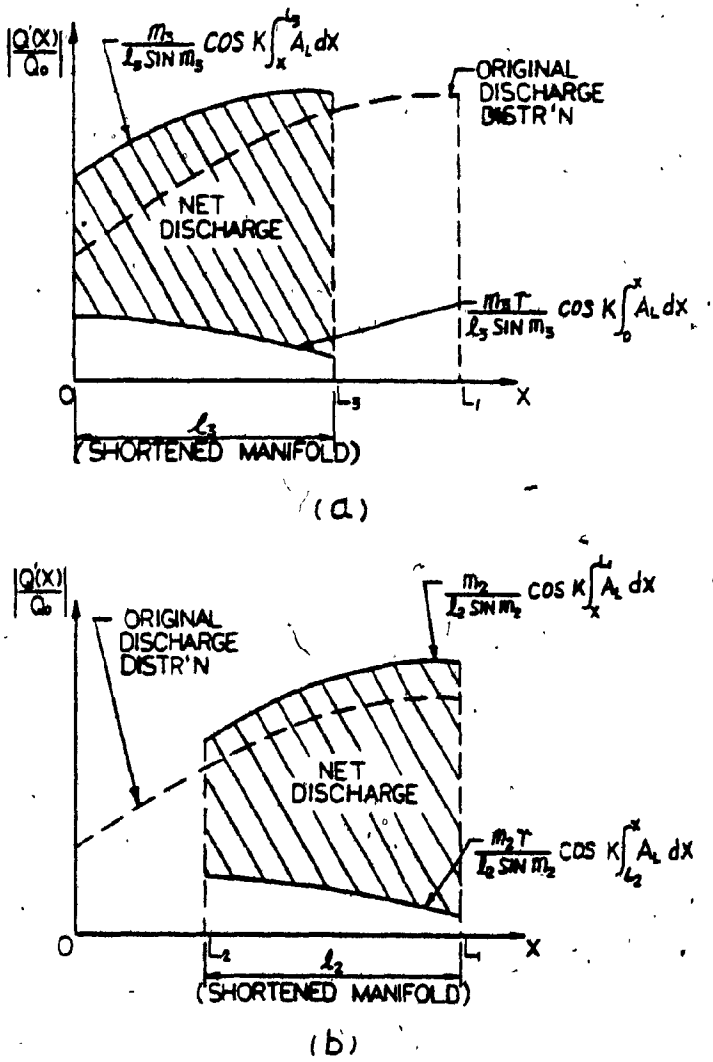

FIG. 4.5 DISCHARGE OF SHORTENED MANIFOLDS WITH A DOWNSTREAM FLOW

CHAPTER V

DISCUSSION OF RESULTS

CHAPTER V

DISCUSSION OF RESULTS

Table 5.1 summarise the test results. Table 5.2 displays the comparison of the test results with the theoretical predictions.

For the case of a closed downstream end, the uniformity of the lateral momentum will not be affected when the manifold is shortened at the upstream end.

For the case of a downstream end being partially opened, the flow behaviour of a section of a manifold remains unchanged if the upstream and downstream flow ratios $\frac{Q(X)}{Q_o}$ of that section are maintained as before. The experimental results of r* (the downstream flow ratio at which the shortened manifold can have a uniform lateral momentum) are close to the predicted values. The values of r_c (the downstream flow ratio at which the manifold will have a zero discharge at the first hole upstream) also agree with the calculated values.

Figures 5.1 to 5.10 show that the theoretical values match the tested data closely when there is no large downstream flow. It is observed from those figures that the experimental lateral momentum is higher at the upstream and lower at the downstream than the theoretical values. This is due to the existence of the friction which creates a pressure drop along the manifold. In the case of a large downstream flow, the discharge at the upstream end is sharply reduced,

and it also means that the pressure recovery head is reduced. Consequently, the effect of friction becomes more obvious and significant.

It is noticed that in Figures 5.1 to 5.10, the distribution of lateral momentum along the first three openings has a wavy profile. This may be caused by the interference due to close hole spacings.

The difference between the calculated discharge and the experimental discharge of each hole is very small. The experimental results verify the analysis which as described in Chapter IV.

The behavious of the discharge of a section of the manifold can be maintained if the flows at the upstream and the downstream of the section remain unchanged. Figure 5.11 shows that the manifold can be elongated in between sections without disturbing the uniformity of the distribution of lateral momentum of each section, provided that the friction loss between sections is small.

Using the analysis presented, one can calculate the discharge of each hole without knowing the hole spacings. The required discharge pattern will then be obtained by adjusting the hole spacings.

Tables in Appendix II summarize the experimental and the calculated results of the discharge and the lateral momentum of the manifolds tested.

TABLE 5.1 SUMMARY OF THE RESULTS OF THE EXPERIMENT

No.of Holes	Hole Number	$\tau = \frac{\text{Downstream Flow}}{\text{Inlet Flow}}$	Characteristics of Momentum Distribution Towards the Downstream
18	1-18	0	Uniform
18	1-18	6.05%	Increases from 85.5% to 114% of the average
16	1-16	0	Decreases from 110% to 93.4% of the average
16	1-16	13.1%	Quite Uniform
16	1-16	50.7%	Increases from 41.6% to 139% of the average
16*	3-18	0	Uniform
16	3-18	13.45%	Increases from 81.7% to 119% of the average
14	1-14	0	Decreases from 129% to 86.4% of the average
14	1-14	25.22%	Quite Uniform
14	1-14	59.23%	Increases from 28.1% to 150% of the average
14*	5-18	0	Uniform
14	5-18	14.25%	Increases from 88% to 120.9% of the average

* Data available in [12].

TABLE 5.2 COMPARISON OF THE EXPERIMENTAL AND ANALYTICAL DOWNSTREAM FLOW RATIOS

No.of Holes	Hole Number	Calculated r	Experimental r
16	1-16	r^* 14.1%	r^* 13%
16	1-16	r_c 50%	r_c 50.7%
14	1-14	r^* 27.9%	r^* 25.2%
14	1-14	r_c 61%	r_c 59.23%

r^* - At uniform discharge momentum.

r_c - At zero discharge at first hole upstream.

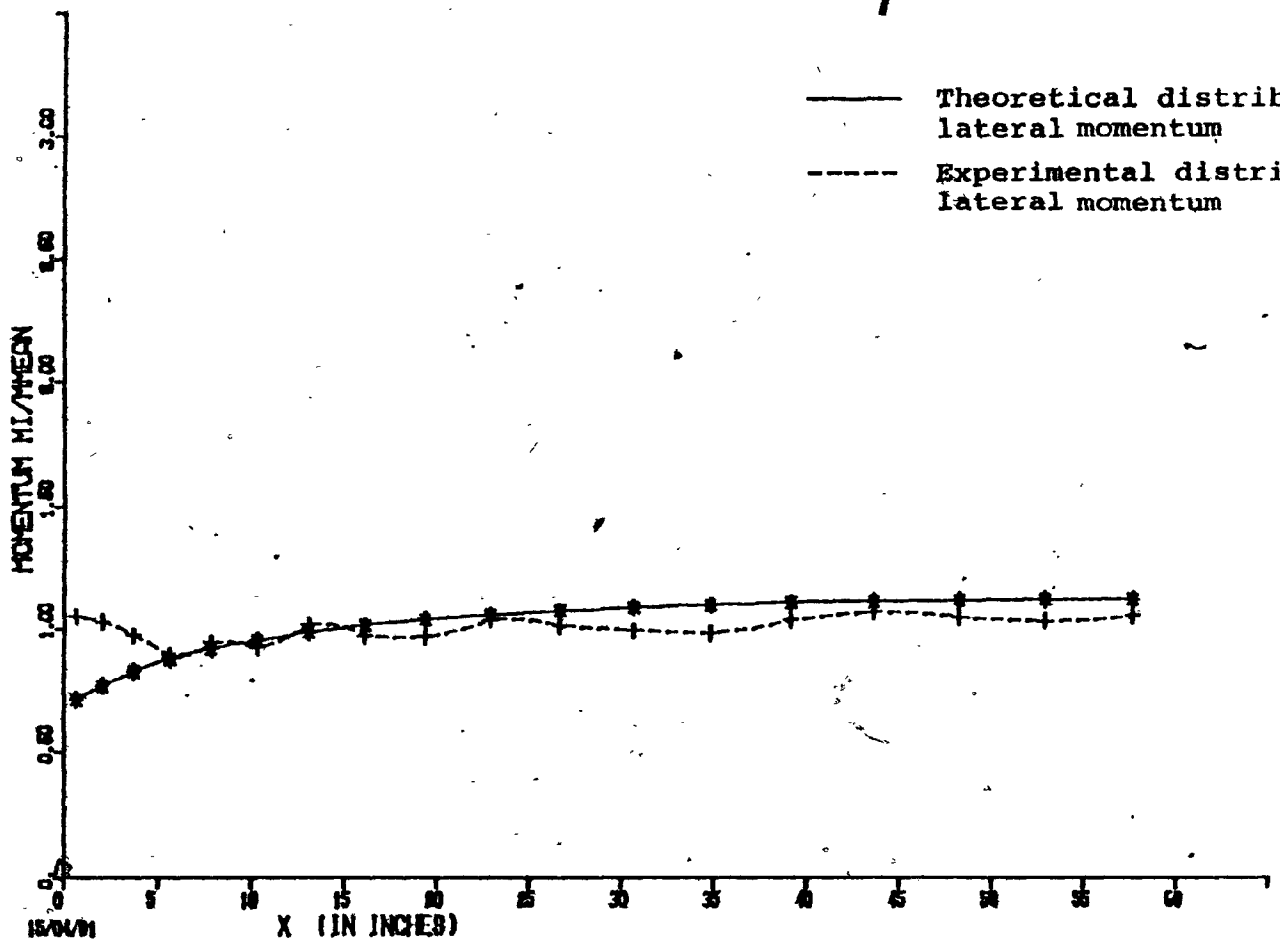

FIG. 5.1 DISTRIBUTION OF LATERAL MOMENTUM FOR THE MANIFOLD WITH HOLES #1 - #18, AND r = 0

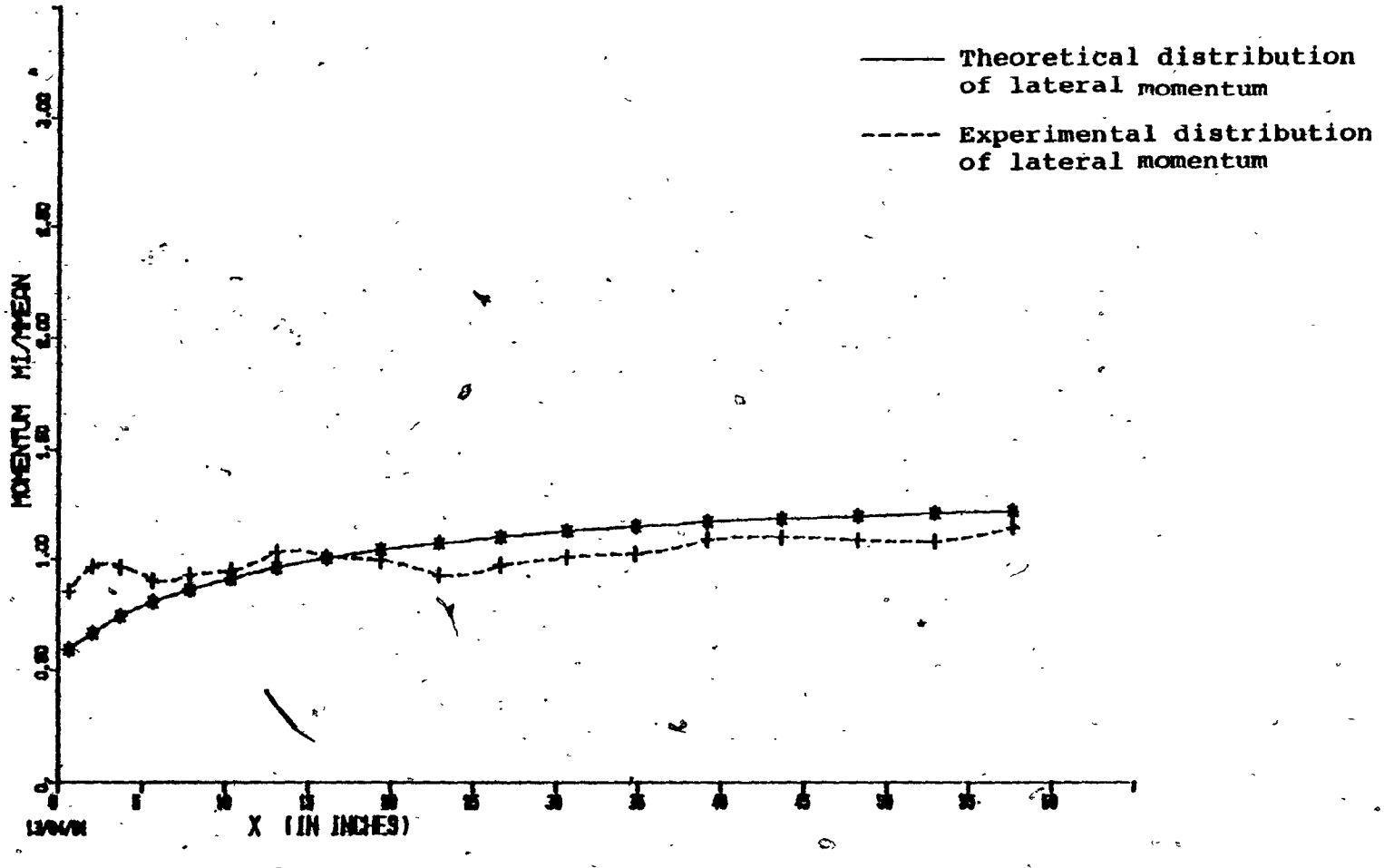

FIG. 5.2 DISTRIBUTION OF LATERAL MOMENTUM FOR THE MANIFOLD WITH HOLES #1 - #18, AND r = 0.0605

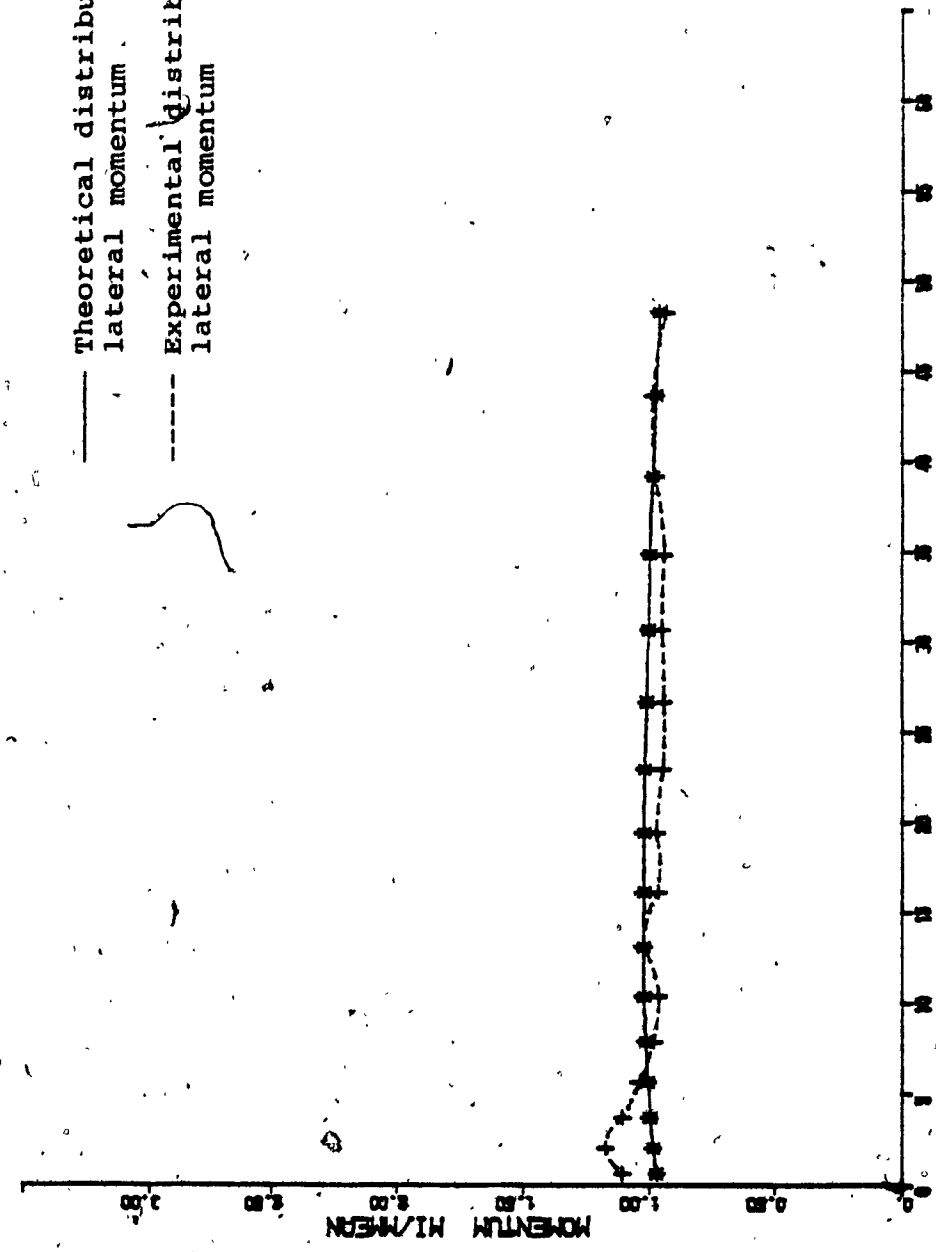

FIG. 5.3 DISTRIBUTION OF LATERAL MOMENTUM FOR THE MANIFOLD WITH HOLES #1 - #16, AND r = 0

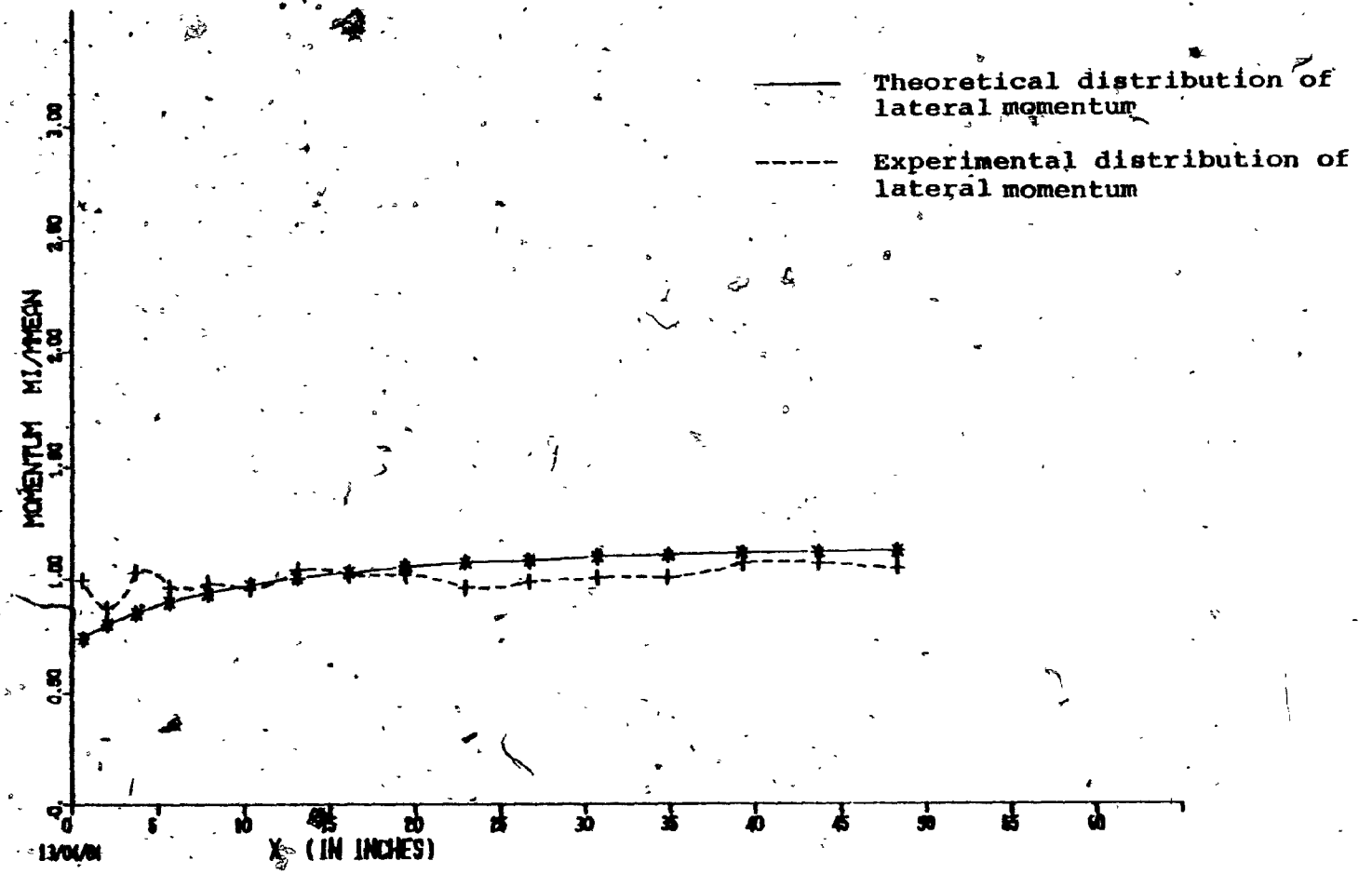

FIG. 5.4 DISTRIBUTION OF LATERAL MOMENTUM FOR THE MANIFOLD WITH HOLES #1 - #16, AND r = 0.131

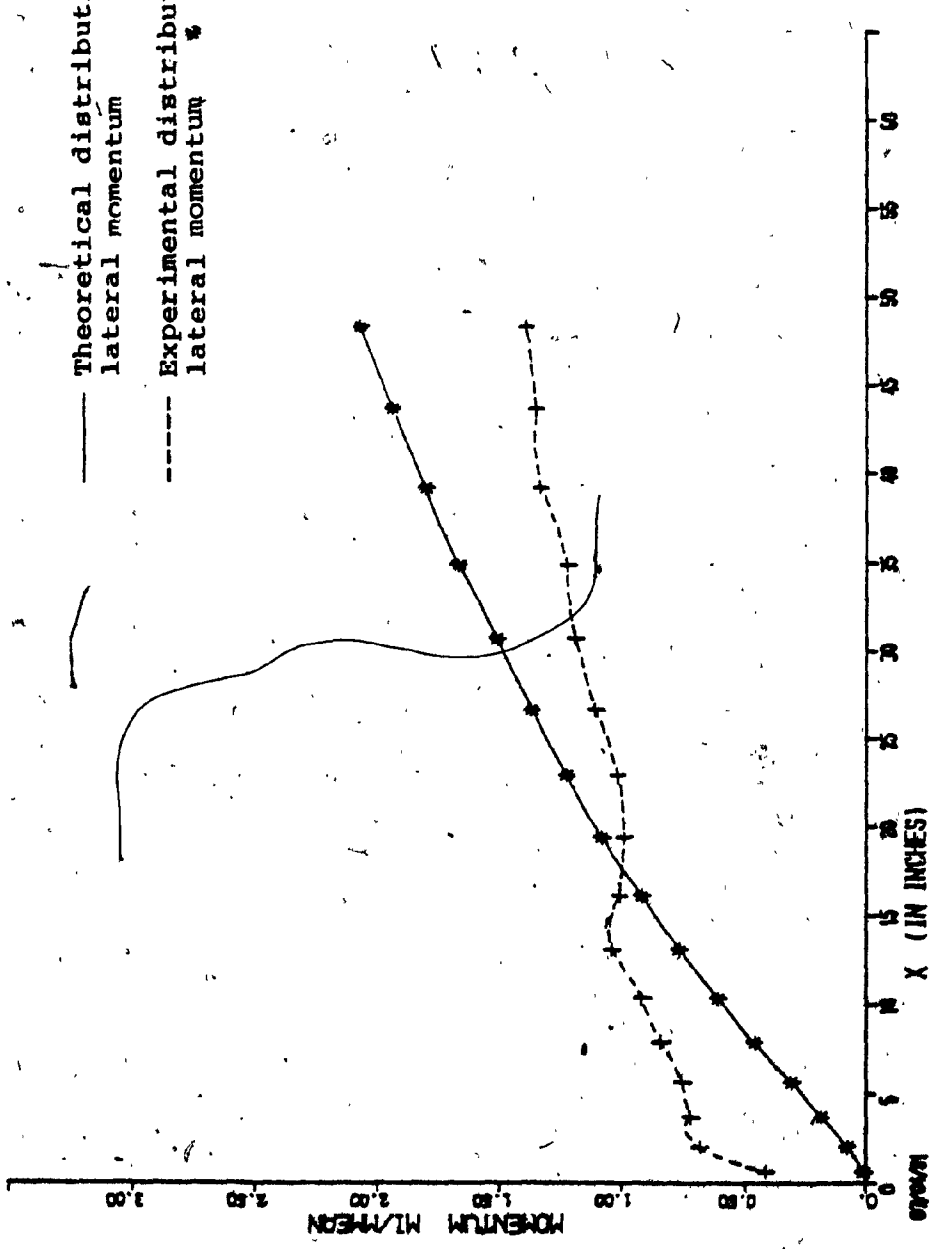

FIG. 5.5 DISTRIBUTION OF LATERAL MOMENTUM FOR THE MANIFOLD WITH HOLES #1 - #16, AND r = 0.507

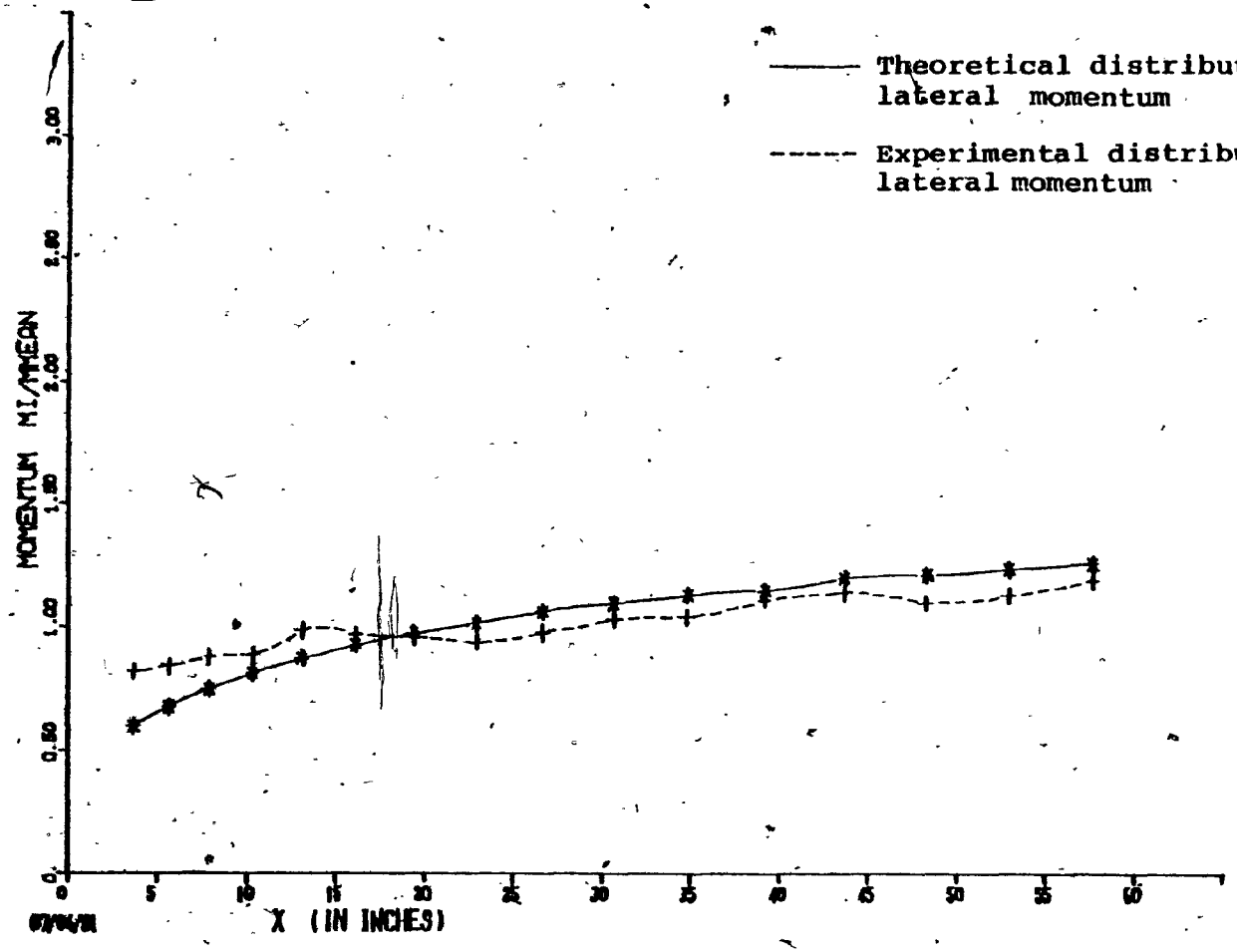

FIG. 5.6 DISTRIBUTION OF LATERAL MOMENTUM FOR THE MANIFOLD WITH HOLES #3 - #18, AND r = 0.1345

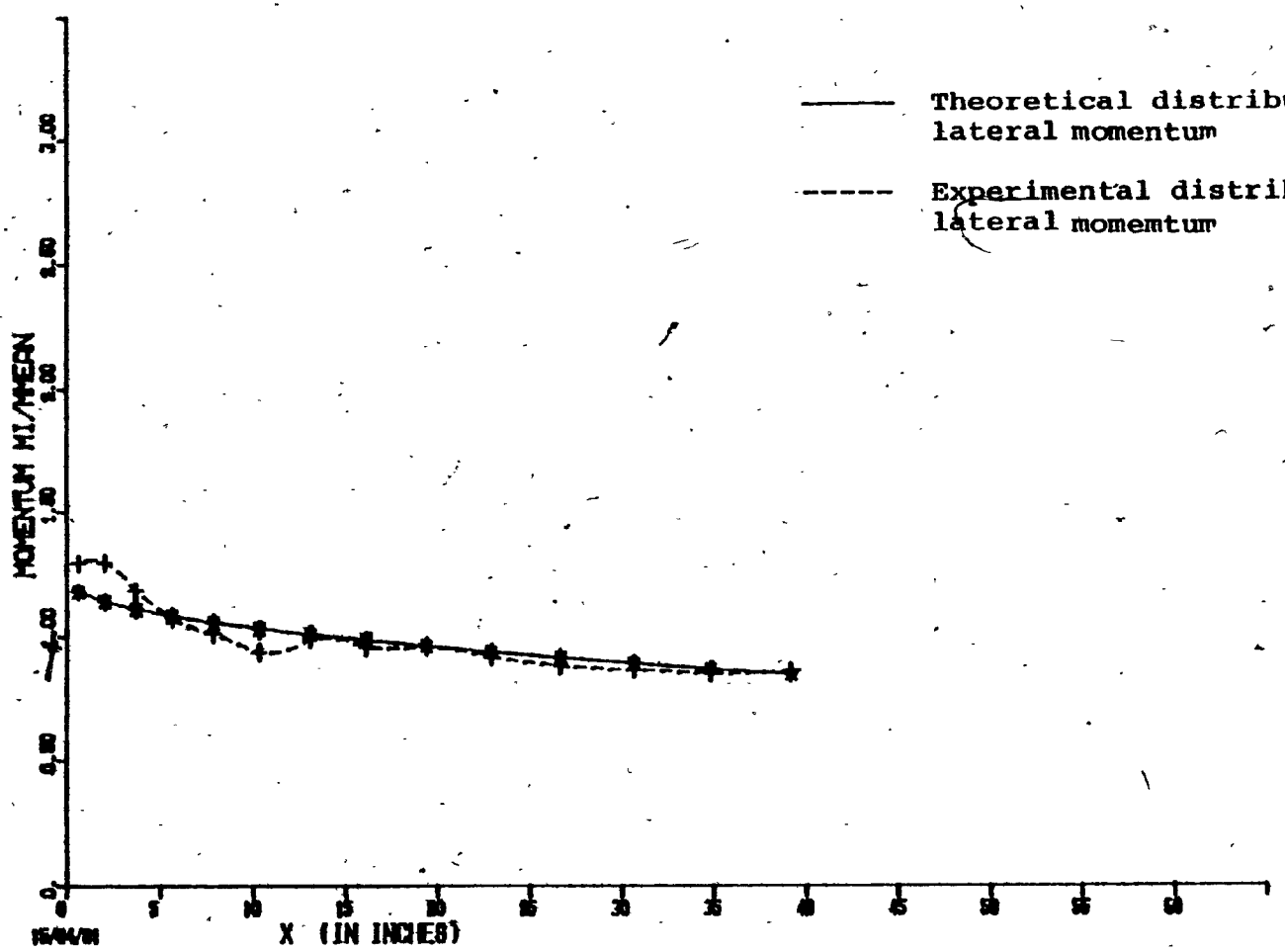

FIG. 5.7 DISTRIBUTION OF LATERAL MOMENTUM FOR THE MANIFOLD WITH HOLES #1 - #14, AND r = 0

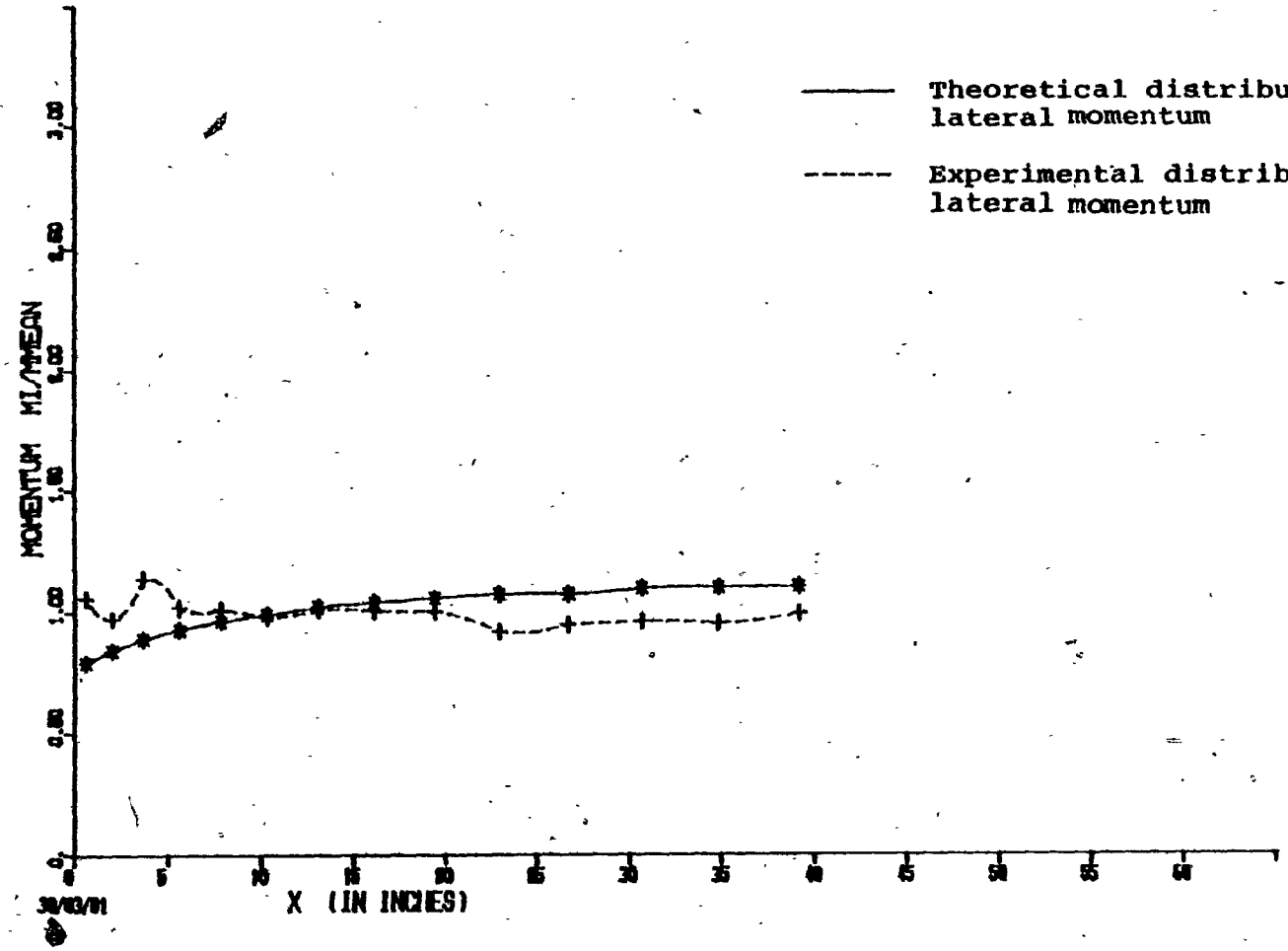

FIG. 5.8 DISTRIBUTION OF LATERAL MOMENTUM FOR THE MANIFOLD WITH HOLES #1 - #14, AND r = 0.263

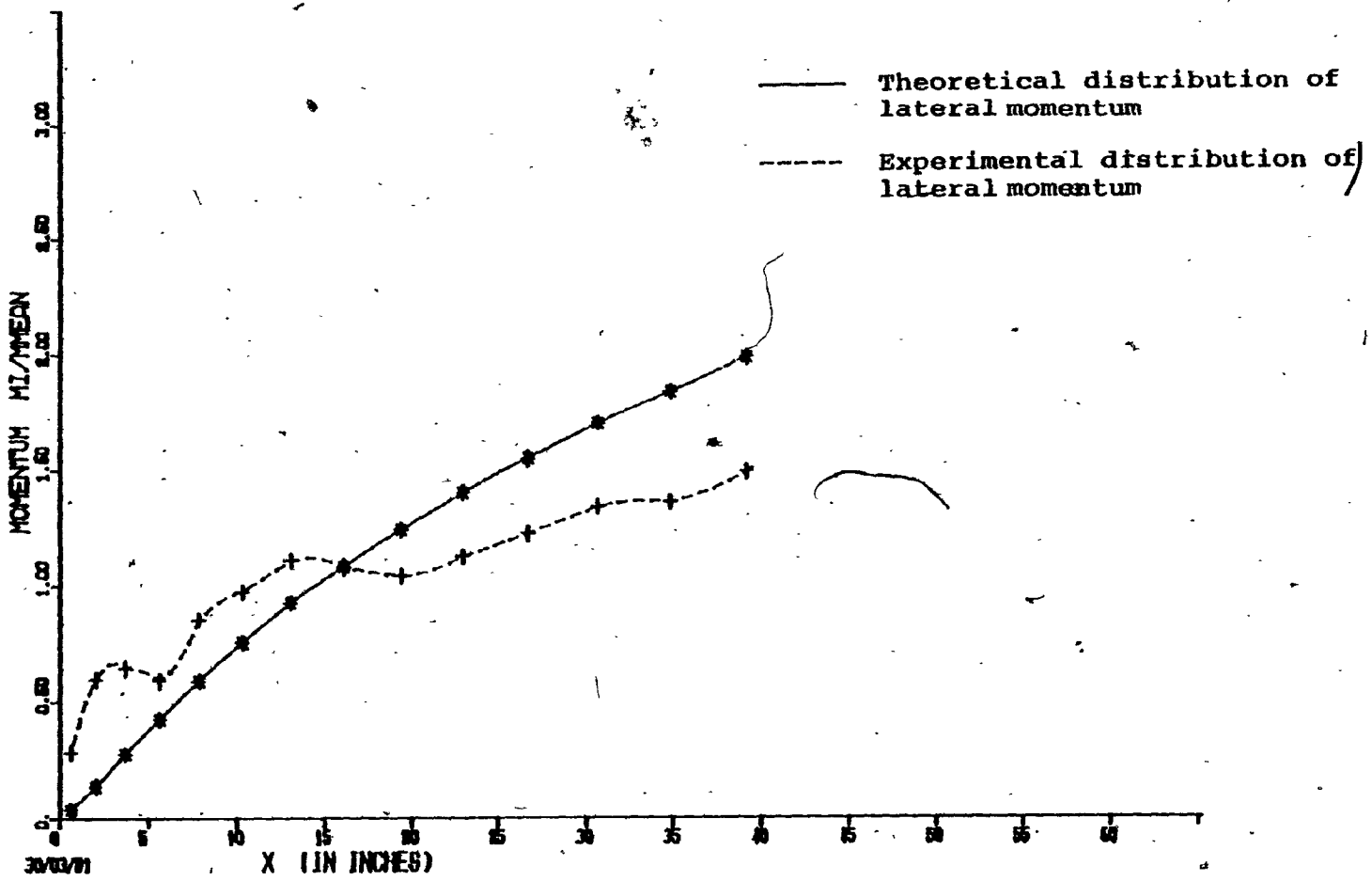

FIG. 5.9 DISTRIBUTION OF LATERAL MOMENTUM FOR THE MANIFOLD WITH HOLES #1 - #14, AND r = 0.592

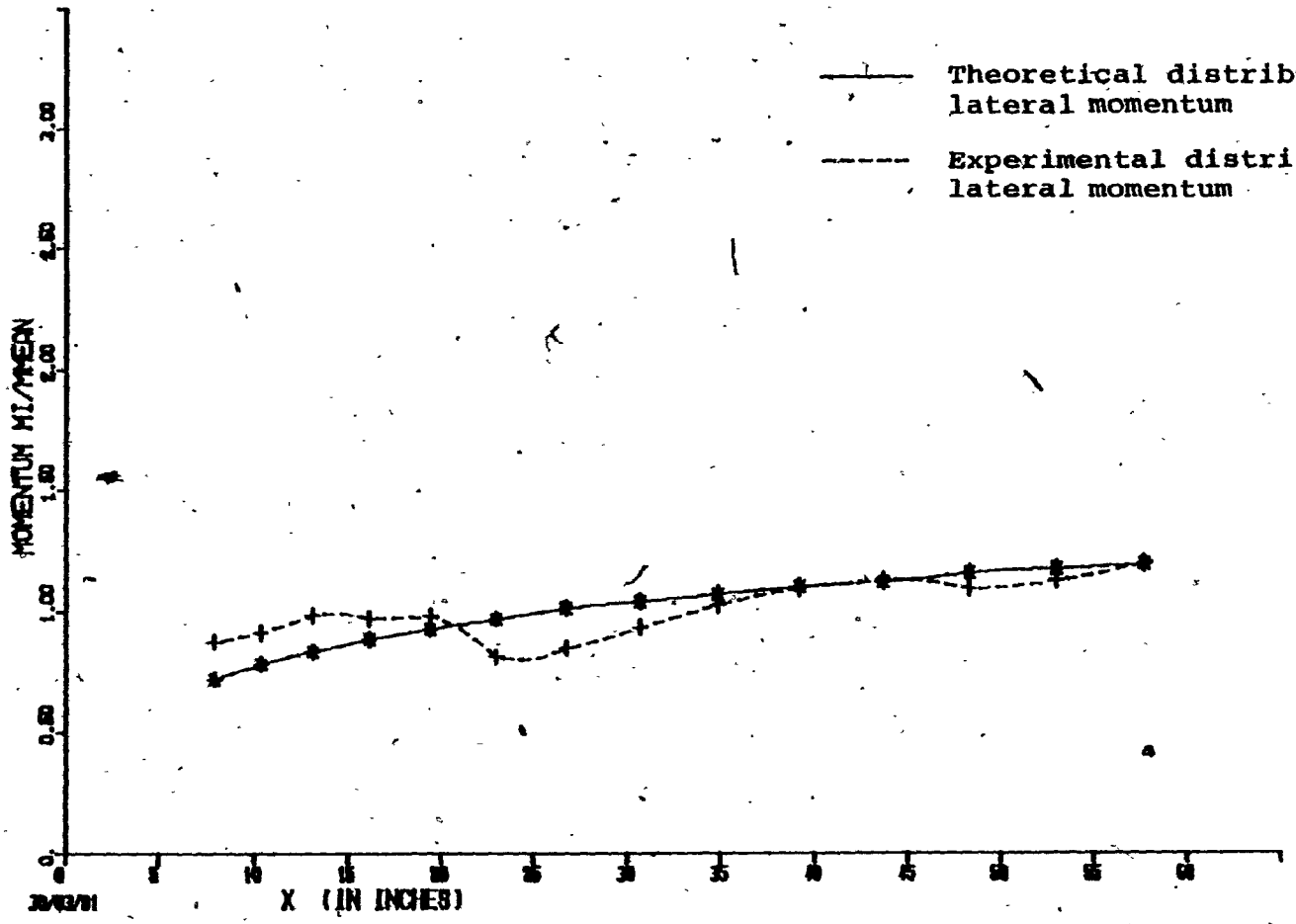

FIG. 5.10 DISTRIBUTION OF LATERAL MOMENTUM FOR THE MANIFOLD WITH HOLES #5 - #18, AND r 0.1425

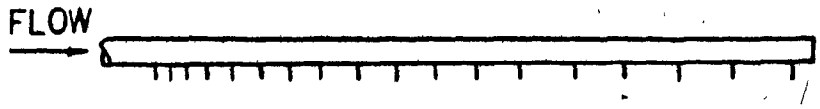

ORIGINAL MANIFOLD

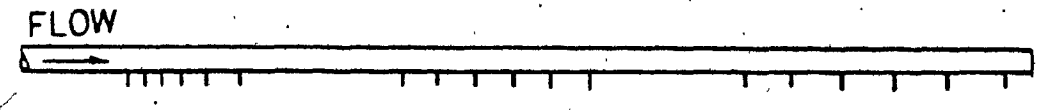

ELONGATED MANIFOLD

FIG. 5.11 ELONGATED MANIFOLD

CHAPTER VI

CONCLUSIONS AND SCOPE FOR FURTHER STUDY

CHAPTER VI

CONCLUSIONS SCOPE FOR FURTHER STUDY

6.1 CONCLUSIONS

The following conclusions can be drawn on the basis of the present study.

1) Friction can be neglected in the design of short manifolds, especially when there is a steep increasing pressure gradient due to closely spaced holes.

2) In the manifold tested, the interference effects due to close hole specing are negligibly small except in the first few holes at the upstream. Thus, any form of lateral discharge can be obtained by simply adjusting the hole spacing. The manifold designer will find this scheme very helpful, espicially in the stage of preliminary design or modification.

3) In handling the discharge more, or less than the design discharge, one can extend or curtail the manifold only at the upstream end in order to avoid disturbing the original flow characteristics and the uniformity of the lateral momentum.

4) The manifold can be elongated in between sections without disturbing the uniformity of the lateral momentum of each section, provided that the friction loss in between sections is small. The elongated manifold will give us a wider spread of the effluents, and will help to dilute the effluents more efficiently.

6.2 SCOPE FOR FURTHER WORK

Even though previous studies [7],[9] showed some experimental data on the interference effects upon the pressure recovery factor and the turning loss coefficient at the branch, more information on the interference effects of hole spacings upon the discharge characteristics of the branch in the manifold is still required for the design and the analysis.

BIBLIOGRAPHY

BIBLIOGRAPHY

[1] Robillard, Luc and Ramamurthy, A.S., "On the Vortex Street of a Counter Jet," J. of Fluids Engineering, ASME, Vol.96, 1974, pp.43-48.

[2] Ramamurthy, A.S., et al, "On the Design of Multi-Port Discharge Diffuser," CSCE, Annual Conference, 1979.

[3] Keller, J.D., "The Manifold Problem," J. of Applied Mech., ASME, March, 1949, pp.77-85.

[4] Dow, W.M., "The Uniform Distribution of a Fluid Flowing Through a Perforated Pipe, J. of Applied Mech., ASME, Vol.72, 1950, pp.431-438.

[5] McNown, J.S., "Mechanics of Manifold Flow," Trans. ASCE, Vol.119, Paper 2714, 1954, pp.1140-1142.

[6] Hortock, J.H., "An Investigation of the Flow in Manifolds With Open and Closed Ends," J. Royal Aeronautical Society, November 1956, pp.749-753.

[7] Haerter, A.A., "Flow Distribution and Pressure Change Along Slotted or Branched Ducts," J. ASHRAE, Vol.5, Nos. 1-6, 1963, pp.47-59.

[8] Vigander, S. et al, "Internal Hydraulics of Thermal Discharge Diffusers," ASCE, J. Hydraulic Div., Vol.96, February 1970, pp.509-527.

[9] Bajura, R.A., "A Model for Flow Distribution in Manifolds," J.of Eng. for Power, ASME, Vol.93, January 1971, pp.7-12.

[10] Berlamont, J. et al, "Solutions for Lateral Outflow in Perforated Conduits," J.Hydraulics Div., ASCE, Vol.99, September 1973, pp.1531-1549.

[11] Hudson, H.E.Jr., et al, "Dividing Flow Manifolds With Square-Edged Laterals," J.Environmental Eng.Div., ASCE, Vol.105, August 1979, pp.745-755.

[12] Ramamurthy, A.S., and Satish, M.G., "Momentum Criteria for Multiport Discharge Diffusers," Internal Report 77-3, Civil Engineering Department, Concordia University, Montreal, Canada.

APPENDIX I

DERIVATION OF DIFFERENTIAL EQUATION FOR MANIFOLD OF UNIFORM LATERAL OPENING

APPENDIX I

DERIVATION OF DIFFERENTIAL EQUATION FOR MANIFOLD OF UNIFORM LATERAL OPENING

The general equation of manifold flow as derived in [7],[9] is as follows:

$$\frac{1}{\rho}\frac{dP}{dX} + \frac{f}{2D}V^2 + (2-\gamma)V\frac{dV}{dX} = 0 \qquad \text{(A1.1)}$$

where,

P = pressure in manifold

f = coefficient of pipe friction

d = diameter of manifold

γ = pressure regain factor

V = flow speed in manifold

ρ = flow

For short manifolds, the friction is neglected. Then Equation (A1.1) becomes

$$\frac{1}{\rho}\frac{dP}{dX} + (2-\gamma)V\frac{dV}{dX} = 0 \qquad \text{(A1.2)}$$

The Bernoulli equation for the flow at the branch

$$\frac{(P-Pr)}{\rho} = \frac{H_v^2}{2} \qquad \text{(A1.3)}$$

where,

v = speed of lateral discharge.

Pr = pressure outside the branch

H = flow resistance at the branch

The continuity equation

$$v = -\frac{dV}{dX}\frac{A}{A_L} \qquad \text{(A1.4)}$$

where,

A_L = lateral area per unit length

Substitute Equation (A1.4) into Equation (A1.3), then differentiate the equation. Substitute that into Equation (A1.1)

$$\ddot{V} + M^2V = 0$$

or

$$\ddot{Q} + M^2Q = 0 \qquad \text{(A1.5)}$$

where,

Q = flow in manifold

$$M = \sqrt{\frac{2-\gamma}{H}}\frac{A_L}{A}$$

The solution for Equation (A1.5) is as follows:

$$Q = a \cos MX + b \sin MX \qquad \text{(A1.6)}$$

For the case of a closed downstream end, at:

$$X = 0 \qquad Q = Q_o$$

$$X = L \qquad Q = 0$$

$$Q(X)\Big|_C = \frac{Q_o}{\sin ML} \sin ML\left(1-\frac{X}{L}\right) \qquad (A1.7)$$

$$Q'(X)\Big|_C = -\frac{MQ_o}{\sin ML} \cos ML\left(1-\frac{X}{L}\right) \qquad (A1.8)$$

where,

Subscript C is for the case of closed downstream end.

For the case of downstream end partially opened

$$X = 0, \qquad Q = Q_o$$

$$X = L, \qquad Q = rQ_o$$

Therefore,

$$Q(X)\Big|_o = \frac{Q_o}{\sin ML} \left[\sin ML\left(1-\frac{X}{L}\right) + r \sin ML\left(1-\frac{X}{L}\right)\right] \qquad (A1.9)$$

$$Q'(X)\Big|_o = -\frac{MQ_o}{\sin ML} \left[\cos ML\left(1-\frac{X}{L}\right) - r \cos M\,\frac{X}{L}\right] \qquad (A1.10)$$

If r is being increased to r_c such that $Q'(0) = 0$, from Equation (A1.10)

$$r_c = \cos ML = \cos \sqrt{\frac{2-\gamma}{H}} \times \frac{A_T}{A} \qquad (A1.11)$$

where,

A_T = total lateral area

For the existing manifold of 1.92" diameter, 5'-0 long with 18 holes of 9/16" diameter, the pressure regain factor $\gamma = 0.9$, and the flow resistance $H = 1.9$, the values of r_c for different numbers of holes are calculated in Table A.1.1.

Let $\frac{X}{L} = \frac{i}{n}$ and $m = ML$,

where,

i = the $i^{\underline{th}}$ number of holes

n = the total number of holes

Equations (A1.7) to (A1.10) can be expressed as follows:

$$Q(i)\Big|_c = \frac{Q_o}{\sin m} \sin m\,(1-\frac{i}{n}) \qquad \text{(A1.12)}$$

$$Q'(i)\Big|_c = \frac{mQ_o}{L \sin m} \cos m(1-\frac{i}{n}) \qquad \text{(A1.13)}$$

$$Q(i)\Big|_o = \frac{Q_o}{\sin m} [\sin m(1-\frac{i}{n}) + r \sin m \frac{i}{n}] \qquad \text{(A1.14)}$$

$$Q'(i)\Big|_o = -\frac{mQ_o}{L \sin m}[\cos m(1-\frac{i}{n}) - r \cos m\frac{i}{n}] \qquad \text{(A1.15)}$$

where,

Q(i) and Q'(i) are the flow at the rate of change of flow after the i^{th} hole.

Therefore, Q_i at the i^{th} hole will be the average of $Q'_{(i-1)}$ and Q'(i).

The experimental lateral momentum per unit length of each hole calculated is as follows:

$$M_i = \rho \frac{q_i^2}{a_i} \frac{1}{S_i} \qquad \text{(A1.16)}$$

where,

M_i = lateral momentum per unit length at the i^{th} hole

q_i = discharge at the i^{th} hole

a_i = cross-sectional area of the i^{th} hole

S_i = spacing of the i^{th} hole.

TABLE A1.1 VALUES OF r_c FOR DIFFERENT NUMBERS OF HOLES

No. of Holes	$\frac{A_T}{A}$	r_c
18	1.545	0.385
16	1.373	0.502
14	1.2	0.611

APPENDIX II

THEORETICAL AND EXPERIMENTAL RESULTS

TABLE A2-1 THEORETICAL AND EXPERIMENTAL RESULTS FOR A MANIFOLD WITH 18 HOLES AND CLOSED DOWNSTREAM END, r = 0

Hole No. (i)	X/L	Theoretical Q_i/Q_o	Experimental Q_i/Q_o	Flow in i^{th} hole Q_i/Q_o Theoretical	Flow in i^{th} hole Q_i/Q_o Experimental	Momentum per unit length Theoretical M_i/M mean	Momentum per unit length Experimental M_i/M mean
	0	1	1				
1				0.0294	0.036	0.714	1.053
	1/18	0.9706	0.964				
2				0.0334	0.039	0.769	1.031
	2/18	0.9372	0.925				
3				0.0375	0.041	0.827	0.973
	3/18	0.8997	0.884				
4				0.0414	0.042	0.878	0.888
	4/18	0.8583	0.842				
5				0.045	0.046	0.917	0.942
	5/18	0.8133	0.796				
6				0.0484	0.048	0.951	0.920
	6/18	0.7649	0.748				
7				0.0517	0.053	0.985	1.018
	7/18	0.7132	0.695				
8				0.0548	0.054	1.015	0.969
	8/18	0.6584	0.641				
9				0.0576	0.056	1.039	0.965
	9/18	0.6008	0.585				
10				0.0601	0.060	1.057	1.036
	10/18	0.5407	0.525				

(continued)

TABLE A2-1 THEORETICAL AND EXPERIMENTAL RESULTS FOR A MANIFOLD WITH 18 HOLES AND CLOSED DOWNSTREAM END, r = 0

Hole No.(i)	X/L	Theoretical Q_i/Q_o	Experimental Q_i/Q_o	Flow in i^{th} hole Q_i/Q_o Theoretical	Flow in i^{th} hole Q_i/Q_o Experimental	Momentum per unit length Theoretical M_i/M mean	Momentum per unit length Experimental M_i/M mean
11	11/18	0.4783	0.464	0.0624	0.061	1.074	1.009
12	12/18	0.4138	0.402	0.645	0.062	1.089	0.99
13	13/18	0.3476	0.339	0.0662	0.063	1.099	0.979
14	14/18	0.2798	0.273	0.0678	0.066	1.111	1.035
15	15/18	0.2107	0.205	0.0689	0.068	1.114	1.068
16	16/18	0.1411	0.137	0.0698	0.068	1.118	1.044
17	17/18	0.707	0.069	0.0704	0.068	1.121	1.028
18	18/18	0.0	0.0	0.0707	0.069	1.122	1.051

TABLE A2-2 THEORETICAL AND EXPERIMENTAL RESULTS FOR A MANIFOLD WITH 18 HOLES AND PARTIALLY OPENED DOWNSTREAM END, r = 0.0605

Hole No.(i)	X/L	Theoretical Q_i/Q_o	Experimental Q_i/Q_o	Flow in i^{th} hole Q_i/Q_o Theoretical	Flow in i^{th} hole Q_i/Q_o Experimental	Momentum per unit length Theoretical M_i/M mean	Momentum per unit length Experimental M_i/M mean
	0	1	1				
1				0.0251	0.0304	0.594	0.855
	1/18	0.9749	0.9696				
2				0.0291	0.0353	0.666	0.963
	2/18	0.9457	0.9343				
3				0.0333	0 0382	0.744	0.962
	3/18	0.9125	0.8961				
4				0.0372	0.0397	0.808	0.904
	4/18	0.8752	0.8565				
5				0.0409	0.0427	0.864	0.928
	5/18	0.8343	0.8137				
6				0.0444	0.0456	0.913	0.946
	6/18	0.7899	0.7682				
7				0.0478	0.0499	0.961	1.031
	7/18	0.7421	0.7182				
8				0.0510	0.0516	1.003	1.008
	8/18	0.6911	0.6667				
9				0.0540	0.0532	1.041	0.992
	9/18	0.6371	0.6135				
10				0.0566	0.0532	1.070	0.927
	10/18	0.5805	0.5603				

(Continued)

TABLE A2-2 THEORETICAL AND EXPERIMENTAL RESULTS FOR A MANIFOLD WITH 18 HOLES AND PARTIALLY OPENED DOWNSTREAM END, r = 0.0605

Hole No.(i)	X/L	Theoretical Q_i/Q_o	Experimental Q_i/Q_o	Flow in i^{th} hole Q_i/Q_o Theoretical	Flow in i^{th} hole Q_i/Q_o Experimental	Momentum per unit length Theoretical M_i/M mean	Momentum per unit length Experimental M_i/M mean
11	11/18	0.5214	0.5043	0.0591	0.0560	1.099	0.971
12	12/18	0.4601	0.4458	0.0614	0.0586	1.126	1.007
13	13/18	0.3968	0.3856	0.0633	0.0602	1.146	1.02
14	14/18	0.3317	0.3223	0.0651	0.0633	1.169	1.085
15	15/18	0.2653	0.2578	0.0664	0.0645	1.181	1.096
16	16/18	0.1978	0.1930	0.0675	0.0648	1.193	1.082
17	17/18	0.1294	0.1278	0.0684	0.0652	1.207	1.078
18	18/18	0.0605	0.0605	0.0689	0.0673	1.216	1.14

TABLE A2-3 THEORETICAL AND EXPERIMENTAL RESULTS FOR A MANIFOLD WITH 16 HOLES AND CLOSED DOWNSTREAM END, r = 0

Hole No.(i)	X/L	Theoretical Q_i/Q_o	Experimental Q_i/Q_o	Flow in i^{th} hole Q_i/Q_o Theoretical	Flow in i^{th} hole Q_i/Q_o Experimental	Momentum per unit length Theoretical M_i/M mean	Momentum per unit length Experimental M_i/M mean
	0	1	1				
1				0.040	0.043	0.971	1.1
	1/16	0.9600	0.957				
2				0.0441	0.0485	0.984	1.17
	2/16	0.9159	0.9085				
3				0.048	0.0509	0.996	1.1
	3/16	0.8679	0.8576				
4				0.0517	0.0526	1.005	1.036
	4/16	0.8162	0.805				
5				0.0552	0.0550	1.014	0.982
	5/16	0.7610	0.75				
6				0.0585	0.0570	1.021	0.963
	6/16	0.7025	0.693				
7				0.0614	0.062	1.021	1.02
	7/16	0.6411	0.631				
8				0.0641	0.0623	1.020	0.964
	8/16	0.5770	0.5687				
9				0.0667	0.0655	1.020	0.97
	9/16	0.5103	0.5032				
10				0.0688	0.0667	1.017	0.945
	10/16	0.4415	0.4365				
11				0.0706	0.0685	1.010	0.943
	11/16	0.3709	0.368				

(Continued)

TABLE A2-3 THEORETICAL AND EXPERIMENTAL RESULTS FOR A MANIFOLD WITH 16 HOLES AND CLOSED DOWNSTREAM END, $r = 0$

Hole No. (i)	x/L	Theoretical Q_i/Q_o	Experimental Q_i/Q_o	Flow in i^{th} hole Q_i/Q_o Theoretical	Flow in i^{th} hole Q_i/Q_o Experimental	Momentum per unit length Theoretical M_i/M mean	Momentum per unit length Experimental M_i/M mean
12	12/16	0.2987	0.2973	0.0722	0.0707	1.003	0.95
13	13/16	0.2251	0.2255	0.0736	0.0718	0.998	0.94
14	14/16	0.1506	0.1509	0.0745	0.0746	0.985	0.978
15	15/16	0.0755	0.0748	0.0751	0.0761	0.972	0.986
16	16/16	0.0	0.0	0.0755	0.0748	0.962	0.934

TABLE A2-4 THEORETICAL AND EXPERIMENTAL RESULTS FOR A MANIFOLD WITH 16 HOLES AND PARTIALLY OPENED END, r = 0.131

Hole No.(i)	x/L	Theoretical Q_i/Q_o	Experimental Q_i/Q_o	Flow in i^{th} hole Q_i/Q_o Theoretical	Flow in i^{th} hole Q_i/Q_o Experimental	Momentum per unit length Theoretical M_i/M mean	Momentum per unit length Experimental M_i/M mean
	0	1	1				
1	1/16	0.9699	0.9648	0.0301	0.0352	0.741	0.994
2	2/16	0.9356	0.9286	0.0343	0.0362	0.803	0.874
3	3/16	0.8974	0.8862	0.0382	0.0424	0.851	1.029
4	4/16	0.8554	0.8422	0.0421	0.0440	0.899	0.962
5	5/16	0.8096	0.7950	0.0457	0.0472	0.937	0.979
6	6/16	0.7604	0.7458	0.0492	0.0492	0.974	0.954
7	7/16	0.708	0.6919	0.0524	0.0539	1.003	1.038
8	8/16	0.6526	0.6361	0.0554	0.0557	1.027	1.017
9	9/16	0.5944	0.5782	0.0583	0.0579	1.054	1.017
10	10/16	0.5336	0.5235	0.0608	0.0580	1.072	0.959
11	11/16	0.4707	0.4629	0.0629	0.0607	1.081	0.985
12	12/16	0.4056	0.3999	0.0651	0.0629	1.099	1.003

(Continued)

TABLE A2-4 THEORETICAL AND EXPERIMENTAL RESULTS FOR A MANIFOLD WITH 16 HOLES AND PARTIALLY OPENED END, r 0.131

Hole No.(i)	L/X	Theoretical Q_i/Q_o	Experimental Q_i/Q_o	Flow in i^{th} hole Q_i/Q_o Theoretical	Flow in i^{th} hole Q_i/Q_o Experimental	Momentum per unit length Theoretical M_i/M mean	Momentum per unit length Experimental M_i/M mean
13				0.0667	0.0643	1.105	1.003
	13/16	0.3389	0.3357				
14				0.0682	0.0674	1.114	1.066
	14/16	0.2707	0.2683				
15				0.0693	0.0684	1.117	1.066
	15/16	0.2014	0.1998				
16				0.0703	0.0687	1.124	1.047
	16/16	0.1310	0.1310				

TABLE A2-5 THEORETICAL AND EXPERIMENTAL RESULTS FOR A MANIFOLD WITH 16 HOLES AND PARTIALLY OPENED END, r = 0.507

Hole No.(i)	X/L	Theoretical Q_i/Q_o	Experimental Q_i/Q_o	Flow in i^{th} hole Q_i/Q_o Theoretical	Flow in i^{th} hole Q_i/Q_o Experimental	Momentum per unit length Theoretical M_i/M mean	Momentum per unit length Experimental M_i/M mean
	0	1	1				
1	1/16	0.9983	0.987	0.0017	0.0127	0.007	0.416
2	2/16	0.9923	0.969	0.006	0.0179	0.073	0.687
3	3/16	0.9820	0.949	0.0103	0.0199	0.1845	0.727
4	4/16	0.9676	0.928	0.0144	0.0218	0.3140	0.761
5	5/16	0.949	0.903	0.0186	0.0245	0.4633	0.847
6	6/16	0.9264	0.876	0.0226	0.0269	0.6143	0.918
7	7/16	0.8998	0.846	0.0266	0.0301	0.7713	1.042
8	8/16	0.8695	0.815	0.0303	0.0309	0.9174	1.608
9	9/16	0.8353	0.783	0.0342	0.0318	1.0828	0.988
10	10/16	0.7977	0.750	0.0376	0.0333	1.2236	1.014
11	11/16	0.7567	0.714	0.041	0.0359	1.3709	1.109
12	12/16	0.7125	0.676	0.0442	0.0382	1.5133	1.189

(Continued)

TABLE A2-5 THEORETICAL AND EXPERIMENTAL RESULTS FOR A MANIFOLD WITH 16 HOLES AND PARTIALLY OPENED END, r = 0.507

Hole No.(i)	x/L	Theoretical Q_i/Q_o	Experimental Q_i/Q_o	Flow in i^{th} hole Q_i/Q_o Theoretical	Flow in i^{th} hole Q_i/Q_o Experimental	Momentum per unit length Theoretical M_i/M mean	Momentum per unit length Experimental M_i/M mean
13	13/16	0.6651	0.637	0.0479	0.0395	1.6664	1.22
14	14/16	0.6150	0.594	0.501	0.0420	1.7942	1.332
15	15/16	0.5622	0.552	0.0528	0.0429	1.9357	1.349
16	16/16	0.507	0.507	0.0552	0.0441	2.0689	1.392

TABLE A2-6 THEORETICAL AND EXPERIMENTAL RESULTS FOR A MANIFOLD WITH 16 HOLES AND PARTIALLY OPENED DOWNSTREAM END, r = 0.1345

Hole No.(i)	X/L	Theoretical Q_i/Q_o	Experimental Q_i/Q_o	Flow in i^{th} hole Q_i/Q_o Theoretical	Flow in i^{th} hole Q_i/Q_o Experimental	Momentum per unit length Theoretical M_i/M mean	Momentum per unit length Experimental M_i/M mean
	0	1.0	1.0				
3				0.0299	0.0349	0.602	0.817
	1/16	0.9701	0.9651				
4				0.034	0.038	0.678	0.842
	2/16	0.9362	0.9271				
5				0.0380	0.0414	0.748	0.88
	3/16	0.8982	0.8857				
6				0.0418	0.0439	0.812	0.89
	4/16	0.8564	0.8418				
7				0.0455	0.0485	0.873	0.99
	5/16	0.8109	0.7933				
8				0.049	0.0502	0.929	0.97
	6/16	0.7619	0.7431				
9				0.0522	0.0519	0.976	0.96
	7/16	0.7097	0.6912				
10				0.0551	0.053	1.017	0.94
	8/16	0.6546	0.6382				
11				0.0581	0.0558	1.065	0.98
	9/16	0.5965	0.5824				
12				0.0605	0.0588	1.097	1.03
	10/16	0.5360	0.5236				
13				0.0628	0.0604	1.132	1.04
	11/16	0.4732	0.4632				
14				0.0645	0.0637	1.151	1.11
	12/16	0.4087	0.3995				

(Continued)

TABLE A2-6 THEORETICAL AND EXPERIMENTAL RESULTS FOR A MANIFOLD WITH 16 HOLES AND PARTIALLY OPENED DOWNSTREAM END, r = 0.1345

Hole No.(i)	X/L	Theoretical Q_i/Q_o	Experimental Q_i/Q_o	Flow in i^{th} hole Q_i/Q_o Theoretical	Flow in i^{th} hole Q_i/Q_o Experimental	Momentum per unit length Theoretical M_i/M mean	Momentum per unit length Experimental M_i/M mean
15	13/16	0.3418	0.3341	0.0669	0.0654	1.203	1.14
16	14/16	0.2738	0.2691	0.0680	0.0650	1.215	1.1
17	15/16	0.2046	0.2028	0.0692	0.0663	1.240	1.13
18	16/16	0.1345	0.1345	0.0701	0.0683	1.263	1.19

TABLE A2-7 THEORETICAL AND EXPERIMENTAL RESULTS FOR A MANIFOLD WITH 14 HOLES AND CLOSED DOWNSTREAM END, r = 0

Hole No.(i)	X/L	Theoretical Q_i/Q_o	Experimental Q_i/Q_o	Flow in i^{th} hole Q_i/Q_o Theoretical	Flow in i^{th} hole Q_i/Q_o Experimental	Momentum per unit length M_i/M mean Theoretical	Momentum per unit length M_i/M mean Experimental
	0	1	1				
1				0.0525	0.0552	1.175	1.29
	1/14	0.9475	0.9448				
2				0.0565	0.0606	1.136	1.293
	2/14	0.8910	0.8842				
3				0.0603	0.0622	1.105	1.18
	3/14	0.8307	0.822				
4				0.0638	0.0644	1.077	1.07
	4/14	0.7669	0.7576				
5				0.0671	0.066	1.053	1.01
	5/14	0.6998	0.6916				
6				0.070	0.0672	1.029	0.939
	6/14	0.6298	0.6244				
7				0.0728	0.0725	1.007	0.992
	7/14	0.5570	0.5519				
8				0.0751	0.0745	0.985	0.958
	8/14	0.4819	0.4774				
9				0.0771	0.0774	0.963	0.961
	9/14	0.4048	0.40				
10				0.0789	0.0753	0.9405	0.919
	10/14	0.3259	0.3247				
11				0.0802	0.0793	0.9175	0.883
	11/14	0.2451	0.2455				

(Continued)

TABLE A2-7 THEORETICAL AND EXPERIMENTAL RESULTS FOR A MANIFOLD WITH 14 HOLES AND CLOSED DOWNSTREAM END, r = 0

Hole No.(i)	X/L	Theoretical Q_i/Q_o	Experimental Q_i/Q_o	Flow in i^{th} hole Q_i/Q_o Theoretical	Flow in i^{th} hole Q_i/Q_o Experimental	Momentum per unit length Theoretical M_i/M mean	Momentum per unit length Experimental M_i/M mean
12				0.0813	0.0805	0.894	0.867
	12/14	0.1644	0.115				
13				0.082	0.0814	0.871	0.85
	13/14	0.0824	0.0836				
14				0.0824	0.0836	0.847	0.864
	14/14	0.0	0.0				

TABLE A2-8 THEORETICAL AND EXPERIMENTAL RESULTS FOR A MANIFOLD WITH 14 HOLES AND PARTIALLY OPENED DOWNSTREAM END, r = 0.253

Hole No.(i)	X/L	Theoretical Q_i/Q_o	Experimental Q_i/Q_o	Flow in i^{th} hole Q_i/Q_o Theoretical	Flow in i^{th} hole Q_i/Q_o Experimental	Momentum per unit length Theoretical M_i/M mean	Momentum per unit length Experimental M_i/M mean
	0	1	1				
1				0.0316	0.0363	0.791	1.058
	1/14	0.9684	0.9637				
2				0.357	0.0373	0.842	0.973
	2/14	0.9326	0.9264				
3				0.0397	0.0438	0.890	1.14
	3/14	0.8929	0.8826				
4				0.0435	0.0457	0.930	1.023
	4/14	0.8929	0.8826				
5				0.0471	0.0483	0.969	1.014
	5/14	0.8023	0.7886				
6				0.0505	0.0486	0.993	0.983
	6/14	0.7519	0.7400				
7				0.0538	0.0549	1.024	1.011
	7/14	0.6981	0.6851				
8				0.0567	0.0568	1.0423	1.007
	8/14	0.6414	0.6283				
9				0.0594	0.0598	1.0597	1.005
	9/14	0.5821	0.5694				
10				0.0619	0.0558	1.076	0.92
	10/14	0.5202	0.5136				
11				0.0638	0.0620	1.077	0.95
	11/14	0.4563	0.4515				

(Continued)

TABLE A2-8 THEORETICAL AND EXPERIMENTAL RESULTS FOR A MANIFOLD WITH 14 HOLES AND PARTIALLY OPENED DOWNSTREAM END, r = 0.253

Hole No.(i)	X/L	Theoretical Q_i/Q_o	Experimental Q_i/Q_o	Flow in i^{th} hole Q_i/Q_o Theoretical	Flow in i^{th} hole Q_i/Q_o Experimental	Momentum per unit length Theoretical M_i/M mean	Momentum per unit length Experimental M_i/M mean
12	12/14	0.3901	0.3870	0.0662	0.0645	1.101	0.964
13	13/14	0.3224	0.3212	0.0677	0.0658	1.103	0.955
14	14/14	0.2533	0.2533	0.0691	0.0679	1.107	0.993

TABLE A2-9 THEORETICAL AND EXPERIMENTAL RESULTS FOR A MANIFOLD WITH 14 HOLES AND PARTIALLY OPENED DOWNSTREAM END, r = 0.592

Hole No.(i)	X/L	Theoretical Q_i/Q_o	Experimental Q_i/Q_o	Flow in i^{th} hole Q_i/Q_o Theoretical	Flow in i^{th} hole Q_i/Q_o Experimental	Momentum per unit length Theoretical M_i/M mean	Momentum per unit length Experimental M_i/M mean
	0	1	1				
1				0.004	0.0103	0.041	0.281
	1/14	0.996	0.9897				
2				0.008	0.0164	0.138	0.596
	2/14	0.9884	0.973				
3				0.0122	0.0218	0.275	0.694
	3/14	0.9702	0.9548				
4				0.0163	0.019	0.427	0.594
	4/14	0.9599	0.9357				
5				0.0204	0.0242	0.591	0.851
	5/14	0.9396	0.9115				
6				0.0243	0.0274	0.752	0.976
	6/14	0.9153	0.8841				
7				0.0283	0.0307	0.926	1.11
	7/14	0.8869	0.8534				
8				0.0320	0.0316	1.085	1.079
	8/14	0.8847	0.8214				
9				0.0356	0.0322	1.245	1.043
	9/14	0.8193	0.7897				
10				0.0392	0.0347	1.411	1.128
	10/14	0.8014	0.755				
11				0.0424	0.0373	1.5555	1.23
	11/14	0.7377	0.7177				

(Continued)

TABLE A2-9 THEORETICAL AND EXPERIMENTAL RESULTS FOR A MANIFOLD WITH 14 HOLES AND PARTIALLY OPENED DOWNSTREAM END, r = 0.592

Hole No.(i)	x/L	Theoretical Q_i/Q_o	Experimental Q_i/Q_o	Flow in i^{th} hole Q_i/Q_o Theoretical	Flow in i^{th} hole Q_i/Q_o Experimental	Momentum per unit length Theoretical M_i/M mean	Momentum per unit length Experimental M_i/M mean
12				0.0456	0.04	1.708	1.35
	12/14	0.6922	0.6776				
13				0.0485	0.041	1.850	1.37
	13/14	0.6436	0.6363				
14				0.0513	0.044	1.995	1.5
	14/14	1.5903	0.5923				